International Research Journal of Engineering and Technology (IRJET) e-ISSN: 2395-0056
Volume: 07 Issue: 10 | Oct 2020 www.irjet.net p-ISSN: 2395-0072

Extension of the Underlying Theory for Calculating Human head Kinematics for a 3-3-3 Array of Peripherally Positioned Triaxial Linear Accelerometer Comprised Sensor Blocks

Jai Singh[1]

[1]*Biomechanical Engineering Analysis & Research, Inc.*
2060-D Avenida de los Arboles, No. 487, Thousand Oaks, California 91362, USA

Abstract – *There exist a number of quantitative metrics for predicting the probability of occurrence of closed head, inclusive of brain, injury when the human head is subjected to impact load, inertial load or both. The accurate quantification of such metrics constitutes a critical endeavor in situations in which a closed head injury represents an injury of consideration. All commonly employed closed head injury metrics involve one or more head kinematic response measures. The translational acceleration response, when employed, is that of the head center of mass. This specific kinematic response can be directly measured when working with biofidelic human surrogates but cannot be directly measured, in a non-invasive manner, when working with live human test subjects and cadaveric test subjects. A consequence of this fact is that measurements must be taken at peripheral locations and then coupled with the appropriate rigid body dynamics equations in order to determine the response in question. One peripheral array configuration, which has been commonly used within the context of live subject testing, is an array consisting of three peripherally located sensor blocks and with each block consisting of three linear accelerometers arranged in a mutually orthogonal configuration. The original study in which the theoretical development was presented for this specific array involved a key assumption. This assumption was of colocation of the head origin of coordinates and the geometric centroid of the plane formed by the three peripheral sensor block locations. The focus of the author, through the subject work, is the extension of the original theoretical framework by removing this assumption. The validity of this extension is shown by considering two example cases with the first being one for which the assumption holds and the second being for one in which the assumption does not hold.*

***Key Words*: Closed head injury, brain injury, biomechanics, rigid body dynamics, accelerometery**

1. INTRODUCTION

From the scientific perspective, establishing a causal relationship between an event in which a mechanical load is applied to a structure and the development of a failure within or of the structure, at any scale of consideration (e.g. microscopic, macroscopic or both), requires an engineering evaluation that includes, but is not limited to the following components: (a) the development or use of appropriate mathematical modeling methods that deterministically relate the relationship between applied mechanical load(s) to either or both the stresses/strains developed within the structure or the kinematic responses of the structure which are deterministically related to the former; (b) the engineering evaluation of the event (i.e. context) in question in regards to determining the applied loads; (c) evaluating the structural response using the mathematical model(s) from (a) and the applied loads from (b); (d) determining whether or not the quantified structural responses are actually predictive of the specific form of failure in question, would result in some other form of structural failure or result in no structural failure with respect to the scale of the analysis. Within the context of a scientific analysis, the methodology is intransigent to the qualitative description of the constituent material(s) that comprise a structure (i.e. the methodology applies in cases involving traditional engineering materials as well as biological materials). Clearly, the correlative approach of temporal association alone, representing the crystalized instantiation of the *post hoc ergo propter hoc* informal logical fallacy, which is (generally) employed clinically, fails to meet the tenets presented herein.

When the structure under consideration is the human head, inclusive of the constituent osseous, meningeal, vascular and neurological components, and the loading is either an impact load, inertial load, or both, there exist a number of injury criteria that can be used for quantifying the potential for the development of various and specific forms of head injury (i.e. structural damage). These criteria include, but are not limited to, the Gadd Severity Index [1], the Head Injury Criterion [2], the Generalized Acceleration Model for Brain Injury Threshold [3], the Head Impact Power criteria [4] and the Brain Injury Criteria [5]. One commonality across all of these criteria is the explicit formulative and functional basis on the kinematic response of the head. This statement of commonality also clearly holds for simpler criteria based solely on peak or average head center of mass translational acceleration or head rotational acceleration.

In the case of controlled testing involving the use of an appropriate anthropometric test device (ATD), the head frame fixed translational acceleration can directly be measured through the use of a sensor block, located at the

head center of mass, consisting of three linear accelerometers arranged in a mutually orthogonal manner. The placement of linear accelerometers peripheral to the head center of mass, depending upon the configuration, allow for the determination of the head angular acceleration. As an example, the standard configuration employed for the Hybrid III ATD, when used in vehicular collision testing for US safety compliance and assessment purposes, consists of a head center of mass triaxial sensor block coupled with biaxial sensor blocks located at the vertex, front and left side of the ATD head [6]. Excluding the redundant head center of mass triaxial sensor block, the array consists of nine linear accelerometers and is referred to as the nine accelerometer array package (NAAP). The 3-2-2-2 scheme, with each number referencing the number of uniaxial accelerometers present for each sensing block and with the triaxial sensor block not necessarily located at the center of mass, was developed to overcome issues encountered with the use of a theoretical minimum six accelerometer array for situations involving impacts [7]. The geometric configuration of the sensor blocks was a key factor in the array as well as in the development of subsequent arrays based upon the 3-2-2-2 scheme [8].

For controlled testing involving live human subjects, the placement of a sensor block at the head center of mass is clearly an infeasible option. In such a context, all sensor block locations clearly must be peripheral. An option for this situation is the use of the 3-3-3 array [9]. This approach, as indicated by the numbering convention, is predicated upon the use of three linear accelerometers, arranged in a mutually orthogonal configuration, for each of the three peripheral sensing blocks. The original authors, based upon the redundancy in the system, employed a least squares approach to solve the coupled rigid body equations of motion, for the angular acceleration of the instrumentation affixed body (i.e. the head) with respect to the inertial frame of reference. The translational center of mass acceleration was solved directly based upon the geometric configuration of the sensing blocks. Specifically, and serving as a limiting assumption, the object center of mass was taken as being located at the geometric centroid of the peripheral sensor block locations. The theoretical basis for this approach has seen cursory mention in the literature [10] but the approach has seen substantive utilization [11-14].

The equations governing the kinematic response for any object that is a rigid body or that can appropriately be modelled as a rigid body are unchanged, within this scope, based upon the specific instantiation of the object. However, there are certain points specifically related to the human head that are worthy of note. The first is the use of surface landmarks for defining the auriculo-orbital plane known as the Frankfort horizontal plane. This plane is defined by three points consisting of the left orbitale (the inferior osseous margin of the left eye socket) and the two porion points. Each porion point is located at the upper margin of each external auditory meatus and lies on the superior margin of the tragus of each ear. The tragion are used to locate the porion points. The Frankfort horizontal plane has been posited and accepted as the plane most reflective of a 'true' horizontal plane for the head [15]. The validity of this acceptance has been questioned for a number of reasons, including anatomical variability [16]. However, the Frankfort horizontal plane remains important in regards to a reference plane for estimating the location of the center of mass of the head. The literature regarding the relationship between this reference plane, as well as other reference planes, the location of the head center of mass and the methodology employed in developing the relationship between the two has been comprehensively reviewed elsewhere [17]. As an example, Walker and Pontius (1973) place the head center of mass in the mid-sagittal plane and 1.42 ± 0.76 cm anterior and 2.41 ± 1.03 cm superior to the Frankfort horizontal plane location of the external auditory meatus [18].

Having established the salient introductory material, the objective of the subject work can be stated as follows: (1) the extension of the 3-3-3 peripheral accelerometer array approach for determining the center of mass translational acceleration of the head (or any other object that can appropriately be modelled as a rigid body) and head angular acceleration when the array is generated such that the center of mass is not located at the geometrical centroid of the same.

2. THEORY

The derivation of the kinematic relationships that describe the motion of a rigid body can be found in most intermediate and advanced level engineering dynamics texts. Unfortunately, there is a wide diversity when it comes to the conventions employed for naming variables. As a consequence of this fact, it is of substantive utility to derive the governing equations from basic principles. The naming convention employed herein follow that of Jazar (2011) (19) and with the derivation following a previous derivation presented by the author (20). This derivation proceeds by considering a vector, $\boldsymbol{\xi}$, in $\mathbb{R}^n$, where n $\{n : n \in \mathbb{N}, n = 3\}$ denotes the order of Euclidean space under consideration, as expressed in two different rectangular Cartesian characterized frames of reference, A and C. Mathematically, the same entity (i.e. the vector $\boldsymbol{\xi}$) can be alternatively expressed as:

$$ {}^{A}\boldsymbol{\xi} = \sum_{p=1}^{n} {}^{A}\xi_{p}\mathbf{e}_{Ap} \qquad {}^{C}\boldsymbol{\xi} = \sum_{p=1}^{n} {}^{C}\xi_{p}\mathbf{e}_{Cp} \tag{1} $$

In equation (1), $\mathbf{e}_{Ap}$ and $\mathbf{e}_{Cp}$ {p: 1 ≤ p ≤ n} denote the set of orthonormal unit vectors that are associated with the rectangular characterization of the A and C frames of reference, respectively. The scalar terms ${}^{A}\xi_{p}$ and ${}^{C}\xi_{p}$ are the components of the vector $\boldsymbol{\xi}$ projected along the p^{th} unit vector of the A and C frames, respectively. Using the A frame

expression (the following also holds for starting with the C frame expression) and taking the first time derivative:

$$\frac{d}{dt}{}^{A}\boldsymbol{\xi} = \sum_{p=1}^{n}\left(\left(\frac{d}{dt}{}^{A}\xi_p\right)\mathbf{e}_{Ap} + {}^{A}\xi_p\left(\frac{d}{dt}\mathbf{e}_{Ap}\right)\right) \quad (2)$$

Equation (2) allows for the introduction of the concept of a frame-referenced time derivative. When the time derivative is taken with respect to the A frame, the time derivatives of the unit vectors of the A frame are zero-valued. A simple frame-referenced time derivative is defined as one in which the expression and derivative frames are the same. For the two equations under (1):

$$\frac{{}^{A}d}{dt}{}^{A}\boldsymbol{\xi} = {}^{A}\dot{\boldsymbol{\xi}} = \sum_{p=1}^{n}{}^{A}\dot{\xi}_p\mathbf{e}_{Ap} \quad \frac{{}^{C}d}{dt}{}^{C}\boldsymbol{\xi} = {}^{C}\dot{\boldsymbol{\xi}} = \sum_{p=1}^{n}{}^{C}\dot{\xi}_p\mathbf{e}_{Cp} \quad (3)$$

In equation (3), the left superscript on the derivative operator denotes the derivative frame. One may also define a mixed frame-referenced time derivative as one for which the expression and derivative frames differ. Using the A frame as the expression frame and the C frame as the derivative frame:

$$\begin{aligned}\frac{{}^{C}d}{dt}{}^{A}\boldsymbol{\xi} &= \frac{{}^{A}d}{dt}{}^{A}\boldsymbol{\xi} + {}^{A}_{C}\boldsymbol{\omega}_A \times {}^{A}\boldsymbol{\xi} \\ {}^{A}_{C}\dot{\boldsymbol{\xi}} &= {}^{A}\dot{\boldsymbol{\xi}} + {}^{A}_{C}\boldsymbol{\omega}_A \times {}^{A}\boldsymbol{\xi}\end{aligned} \quad (4)$$

In equation (4), ${}^{A}_{C}\dot{\boldsymbol{\xi}}$ denotes the A frame expressed (left superscript) C frame-referenced time derivative (left subscript) of the vector ${}^{A}\square$, ${}^{A}\dot{\boldsymbol{\xi}}$ denotes the A frame expressed A frame-referenced time derivative of the vector ${}^{A}\square$ and ${}^{A}_{C}\boldsymbol{\omega}_A$ denotes the angular velocity vector of the A frame (right subscript), about the C frame (left subscript), expressed in the A frame (left superscript). The vector ${}^{A}\square$ can be any vector such as a position, velocity or acceleration vector (expressed in the A frame). A consequence of this fact is that equation (4) is referred to as the derivative transport theorem. Because the vector cross product is anti-commutative (i.e. **a** x **b** = -**b** x **a**), equation (4) can readily be written as:

$${}^{A}_{C}\dot{\boldsymbol{\xi}} = {}^{A}\dot{\boldsymbol{\xi}} - {}^{A}\boldsymbol{\xi} \times {}^{A}_{C}\boldsymbol{\omega}_A \quad (5)$$

Equation (4) can also be rewritten by noting that the cross-product operation can be replaced by the equivalent vector-matrix product by means of using the skew-symmetric (i.e. antisymmetric) matrix associated with the first vector in the operation times the second vector.

$${}^{A}_{C}\dot{\boldsymbol{\xi}} = {}^{A}\dot{\boldsymbol{\xi}} + {}^{A}_{C}\tilde{\omega}_A\,{}^{A}\boldsymbol{\xi} \quad (6)$$

Where:

$${}^{A}_{C}\tilde{\omega}_A = \begin{bmatrix} 0 & -{}^{A}_{C}\tilde{\omega}_{A-3} & +{}^{A}_{C}\tilde{\omega}_{A-2} \\ +{}^{A}_{C}\tilde{\omega}_{A-3} & 0 & -{}^{A}_{C}\tilde{\omega}_{A-1} \\ -{}^{A}_{C}\tilde{\omega}_{A-2} & +{}^{A}_{C}\tilde{\omega}_{A-1} & 0 \end{bmatrix} \quad (7)$$

The dash followed by a number in the right subscript refers to the corresponding position in the 3 x 1 (column vector) angular velocity vector.

2.1 Inertial and body frames of reference

For the subject work, the ground-fixed frame of reference is sufficient for use as an inertial frame of reference (G frame). This reference frame is characterized as rectangular Cartesian with origin **O** and an orthonormal triad of unit vectors $\mathbf{E}_1$, $\mathbf{E}_2$ and $\mathbf{E}_3$ with corresponding respective coordinate axes **X**, **Y** and **Z**. The head fixed frame of reference is referred to as the body frame (B frame) predicated upon the fact that it is the body, under consideration, that is moving within the inertial frame of reference. This frame of reference is characterized as rectangular Cartesian with origin **o** and an orthonormal triad of unit vectors $\mathbf{e}_1$, $\mathbf{e}_2$ and $\mathbf{e}_3$ with corresponding respective coordinate axes **x**, **y** and **z**. The origin of coordinates of the body frame is taken as being colocated with the static center of mass of the head, thereby making the body frame a central frame. Anatomically, the **x**-axis is parallel to the Frankfort plane and follows the sign convection of +**x** being directed from posterior to anterior. The **z**-axis is orthogonal to the Frankfort plane and follows the sign convention of +**z** directed from inferior to superior. In order for this coordinate system to be a right handed coordinate system, the **y**-axis must be parallel to the Frankfort plane, mutually orthogonal with respect to the other two body frame coordinate axes and following a sign convention of +**y** directed to the left. It should be noted that there exists a second right handed configuration, consisting of a ±□ radian rotation about the +**x**-axis, which is commonly employed in the literature. The transformation between the two coordinate systems requires the simple process of taking the negative value of reported components along the **y**-axis and **z**-axis. Care should be taken to ensure that note is taken of the sign convention employed within any given literature source. With respect to the original reference [9], the G frame is denoted as the laboratory frame and the B frame is denoted as the anatomical frame.

For a point of interest, $\mathbf{p}_k$, the G frame and B frame expressions for the position vector of the point, $\mathbf{r}_k$, can be related by the following:

$${}^{G}\mathbf{r}_k(t) = {}^{G}\mathbf{r}_o(t) + {}^{G}R_B(t)\,{}^{B}\mathbf{r}_k(t) \quad (8)$$

Where ${}^{G}\mathbf{r}_k(t)$ is the G frame expression of the position vector of the point $\mathbf{p}_k$, ${}^{G}\mathbf{r}_o(t)$ is the position of the origin of coordinates of the B frame, expressed in the G frame, ${}^{G}R_B$ is the direction cosine matrix (DCM) that transforms vector coordinates from the B frame (right subscript) to the G frame (left superscript) and ${}^{B}\mathbf{r}_k(t)$ is the B frame expression of the position vector of the point $\mathbf{p}_k$. The DCM is an orthogonal matrix (i.e. $R^{-1} = R^T$). Therefore, the inverse transform, ${}^{B}R_G(t)$, can be obtained from $({}^{G}R_B(t))^{-1} = ({}^{G}R_B(t))^T$. The DCM can be parameterized in a number of ways, including but not

limited to, Euler angles and Cardan angles. Equation (8) can readily be inverted, by algebraic rearrangement, to provide the solution for ${}^{B}\mathbf{r}_k(t)$.

$$\begin{aligned} {}^{B}\mathbf{r}_k(t) &= \left({}^{G}R_B(t)\right)^{-1}\left({}^{G}\mathbf{r}_k(t) - {}^{G}\mathbf{r}_o(t)\right) \\ &= \left({}^{G}R_B(t)\right)^{T}\left({}^{G}\mathbf{r}_k(t) - {}^{G}\mathbf{r}_o(t)\right) \\ &= \left({}^{B}R_G(t)\right)\left({}^{G}\mathbf{r}_k(t) - {}^{G}\mathbf{r}_o(t)\right) \end{aligned} \tag{9}$$

In the following derivation, the explicit dependence on time is not shown. This is solely for the purpose of improving the clarity of presentation. It should be well noted that the appropriate terms are time-varying.

2.2 Derivative kinematics

An important theorem in the development of the derivative kinematics, while not proven here, is that the frame-referenced time derivative of a DCM premultiplied frame-referenced vector is equal to the product of the DCM and the frame-referenced time derivative of the vector. For any two frames A and C:

$$\frac{{}^{C}d}{dt}\left({}^{C}R_A\,{}^{A}\mathbf{r}\right) = {}^{C}R_A\left(\frac{{}^{C}d}{dt}\,{}^{A}\mathbf{r}\right) \tag{10}$$

Taking the first G derivative of equation (8), making use of equations (4) and (10):

$$\begin{aligned} \frac{{}^{G}d}{dt}\,{}^{G}\mathbf{r}_k &= \frac{{}^{G}d}{dt}\left({}^{G}\mathbf{r}_o + {}^{G}R_B\,{}^{B}\mathbf{r}_k\right) \\ &= {}^{G}\dot{\mathbf{r}}_o + {}^{G}R_B\left(\frac{{}^{G}d}{dt}\,{}^{B}\mathbf{r}_k\right) \\ {}^{G}\dot{\mathbf{r}}_k &= {}^{G}\dot{\mathbf{r}}_o + {}^{G}R_B\left({}^{B}\dot{\mathbf{r}}_k + {}^{B}_{G}\boldsymbol{\omega}_B \times {}^{B}\mathbf{r}_k\right) \end{aligned} \tag{11}$$

When the point $\mathbf{p}_k$ is fixed in the body frame (i.e. a body point), its position vector in the body frame, ${}^{B}\mathbf{r}_k(t)$, becomes time-invariant. A consequence of this fact is that the body frame-referenced time derivatives for ${}^{B}\mathbf{r}_k$ become zero-valued. For such a case, equation (11) reduces to the following:

$${}^{G}\dot{\mathbf{r}}_k = {}^{G}\dot{\mathbf{r}}_o + {}^{G}R_B\left({}^{B}_{G}\boldsymbol{\omega}_B \times {}^{B}\mathbf{r}_k\right) \tag{12}$$

For the subject work, the velocity relationship given by equation (12) is the appropriate equation given that each point $\mathbf{p}_k$ is taken as representing the origin of the k^{th} body affixed sensor block. Taking the G derivative of equation (12):

$$\begin{aligned} \frac{{}^{G}d}{dt}\,{}^{G}\dot{\mathbf{r}}_k &= \frac{{}^{G}d}{dt}\,{}^{G}\dot{\mathbf{r}}_o + {}^{G}R_B\left(\frac{{}^{G}d}{dt}\left({}^{B}_{G}\boldsymbol{\omega}_B \times {}^{B}\mathbf{r}_k\right)\right) \\ {}^{G}\ddot{\mathbf{r}}_k &= {}^{G}\ddot{\mathbf{r}}_o + {}^{G}R_B\left(\begin{array}{l}\left(\frac{{}^{G}d}{dt}\,{}^{B}_{G}\boldsymbol{\omega}_B\right)\times {}^{B}\mathbf{r}_k + \\ {}^{B}_{G}\boldsymbol{\omega}_B \times \left(\frac{{}^{G}d}{dt}\,{}^{B}\mathbf{r}_k\right)\end{array}\right) \end{aligned} \tag{13}$$

Expanding the first term in the outer parenthetical on the right side of the second form of equation (13):

$$\begin{aligned} \left(\frac{{}^{G}d}{dt}\,{}^{B}_{G}\boldsymbol{\omega}_B\right)\times {}^{B}\mathbf{r}_k &= \left(\frac{{}^{B}d}{dt}\,{}^{B}_{G}\boldsymbol{\omega}_B + {}^{B}_{G}\boldsymbol{\omega}_B \times {}^{B}_{G}\boldsymbol{\omega}_B\right)\times {}^{B}\mathbf{r}_k \\ &= \left(\frac{{}^{B}d}{dt}\,{}^{B}_{G}\boldsymbol{\omega}_B + \mathbf{0}\right)\times {}^{B}\mathbf{r}_k \\ &= {}^{B}_{G}\dot{\boldsymbol{\omega}}_B \times {}^{B}\mathbf{r}_k \\ &= {}^{B}_{G}\boldsymbol{\alpha}_B \times {}^{B}\mathbf{r}_k \end{aligned} \tag{14}$$

Expanding the second term in the outer parenthetical on the right side of the second form of equation (13):

$$\begin{aligned} {}^{B}_{G}\boldsymbol{\omega}_B \times \left(\frac{{}^{G}d}{dt}\,{}^{B}\mathbf{r}_k\right) &= {}^{B}_{G}\boldsymbol{\omega}_B \times \left(\frac{{}^{B}d}{dt}\,{}^{B}\mathbf{r}_k + {}^{B}_{G}\boldsymbol{\omega}_B \times {}^{B}\mathbf{r}_k\right) \\ &= {}^{B}_{G}\boldsymbol{\omega}_B \times \left(\mathbf{0} + {}^{B}_{G}\boldsymbol{\omega}_B \times {}^{B}\mathbf{r}_k\right) \\ &= {}^{B}_{G}\boldsymbol{\omega}_B \times \left({}^{B}_{G}\boldsymbol{\omega}_B \times {}^{B}\mathbf{r}_k\right) \end{aligned} \tag{15}$$

Substitution of the results from equations (14) and (15) into equation (13) results in the following solution for the G frame expression of the acceleration at $\mathbf{p}_k$.

$${}^{G}\ddot{\mathbf{r}}_k = {}^{G}\ddot{\mathbf{r}}_o + {}^{G}R_B\left(\begin{array}{l}{}^{B}_{G}\dot{\boldsymbol{\omega}}_B \times {}^{B}\mathbf{r}_k + \\ {}^{B}_{G}\boldsymbol{\omega}_B \times \left({}^{B}_{G}\boldsymbol{\omega}_B \times {}^{B}\mathbf{r}_k\right)\end{array}\right) \tag{16}$$

The body frame solution is obtained by premultiplying equation (16) by the DCM ${}^{B}R_G$.

$${}^{B}_{G}\ddot{\mathbf{r}}_k = {}^{B}_{G}\ddot{\mathbf{r}}_o + {}^{B}_{G}\dot{\boldsymbol{\omega}}_B \times {}^{B}\mathbf{r}_k + {}^{B}_{G}\boldsymbol{\omega}_B \times \left({}^{B}_{G}\boldsymbol{\omega}_B \times {}^{B}\mathbf{r}_k\right) \tag{17}$$

2.3 Original solution approach

In the original work [9], equation (17) served as the operative equation. This equation was rewritten using equation (5) on the cross product associated with the angular velocity and then converting all cross product operations to the corresponding vector-matrix products. The result of these operations is:

$${}^{B}_{G}\ddot{\mathbf{r}}_k = {}^{B}_{G}\ddot{\mathbf{r}}_o - {}^{B}\tilde{\mathbf{r}}_k\,{}^{B}_{G}\dot{\boldsymbol{\omega}}_B + {}^{B}_{G}\tilde{\omega}_B\left({}^{B}_{G}\tilde{\omega}_B\,{}^{B}\mathbf{r}_k\right) \tag{18}$$

Where the skew-symmetric matrices associated with the position vector ${}^{B}\mathbf{r}_k$ and the angular velocity vector are:

$$ {}^{B}\tilde{\mathbf{r}}_k = \begin{bmatrix} 0 & -{}^{B}r_{k-3} & +{}^{B}r_{k-2} \\ +{}^{B}r_{k-3} & 0 & -{}^{B}r_{k-1} \\ -{}^{B}r_{k-2} & +{}^{B}r_{k-1} & 0 \end{bmatrix} \quad (19) $$

$$ {}^{B}_{G}\tilde{\omega}_{B} = \begin{bmatrix} 0 & -{}^{B}_{G}\tilde{\omega}_{B-3} & +{}^{B}_{G}\tilde{\omega}_{B-2} \\ +{}^{B}_{G}\tilde{\omega}_{B-3} & 0 & -{}^{B}_{G}\tilde{\omega}_{B-1} \\ -{}^{B}_{G}\tilde{\omega}_{B-2} & +{}^{B}_{G}\tilde{\omega}_{B-1} & 0 \end{bmatrix} \quad (20) $$

Equation (18) represents three coupled equations with one equation per sensing axis of the triaxial accelerometer sensor block located at ${}^{B}\mathbf{r}_k$. The term on the left side of the equality is the measured response while the terms on the right side of the equality can be viewed as the modeled response. In the original approach [9], subtracting the measured response from both sides of the equality was taken as not producing a **0** resultant on the left side of the equality. Instead, the resultant was a 3 x 1, small, error vector.

$$ \boldsymbol{\varepsilon}_k = {}^{B}_{G}\ddot{\mathbf{r}}_o - {}^{B}\tilde{\mathbf{r}}_k {}^{B}_{G}\dot{\boldsymbol{\omega}}_B + {}^{B}_{G}\tilde{\omega}_B \left({}^{B}_{G}\tilde{\omega}_B {}^{B}\mathbf{r}_k \right) - {}^{B}_{G}\ddot{\mathbf{r}}_k \quad (21) $$

Because the problem involves three triaxial sensor blocks, the three coupled sets of equations (one set per block), can be collected in the following form:

$$ \left[{}^{B}_{G}\ddot{\mathbf{r}}_o \right] - \left[{}^{B}\tilde{\mathbf{r}} \right] {}^{B}_{G}\dot{\boldsymbol{\omega}}_B + \left[{}^{B}\boldsymbol{\upsilon} \right] = \left[\boldsymbol{\varepsilon} \right] \quad (22) $$

Where:

$$ \left[{}^{B}_{G}\ddot{\mathbf{r}}_o \right]_{9\times 1} = \begin{bmatrix} {}^{B}_{G}\ddot{\mathbf{r}}_o \\ {}^{B}_{G}\ddot{\mathbf{r}}_o \\ {}^{B}_{G}\ddot{\mathbf{r}}_o \end{bmatrix} \quad (23) $$

$$ \left[{}^{B}\tilde{\mathbf{r}} \right]_{9\times 3} = \begin{bmatrix} {}^{B}\tilde{\mathbf{r}}_1 \\ {}^{B}\tilde{\mathbf{r}}_2 \\ {}^{B}\tilde{\mathbf{r}}_3 \end{bmatrix} \quad (24) $$

$$ \left[{}^{B}\boldsymbol{\upsilon} \right]_{9\times 1} = \begin{bmatrix} {}^{B}_{G}\tilde{\omega}_B \left({}^{B}_{G}\tilde{\omega}_B {}^{B}\mathbf{r}_1 \right) - {}^{B}_{G}\ddot{\mathbf{r}}_1 \\ {}^{B}_{G}\tilde{\omega}_B \left({}^{B}_{G}\tilde{\omega}_B {}^{B}\mathbf{r}_2 \right) - {}^{B}_{G}\ddot{\mathbf{r}}_2 \\ {}^{B}_{G}\tilde{\omega}_B \left({}^{B}_{G}\tilde{\omega}_B {}^{B}\mathbf{r}_3 \right) - {}^{B}_{G}\ddot{\mathbf{r}}_3 \end{bmatrix} \quad (25) $$

$$ \left[\boldsymbol{\varepsilon} \right]_{9\times 1} = \begin{bmatrix} \boldsymbol{\varepsilon}_1 \\ \boldsymbol{\varepsilon}_2 \\ \boldsymbol{\varepsilon}_3 \end{bmatrix} \quad (26) $$

It is instructive to first discuss the solution presented in the original work for the body frame center of mass translational acceleration prior to presenting the solution for the angular acceleration. Because it was assumed that the three sensor blocks are positioned such that the center of mass lies at the geometric centroid of the (triangular) plane formed by the three peripheral positions:

$$ {}^{B}\mathbf{r}_o = \mathbf{0} = \frac{1}{3}\left({}^{B}\mathbf{r}_1 + {}^{B}\mathbf{r}_2 + {}^{B}\mathbf{r}_3 \right) \quad (27) $$

Taking two body frame-referenced derivatives of equation (27):

$$ {}^{B}\ddot{\mathbf{r}}_o = \frac{1}{3}\left({}^{B}\ddot{\mathbf{r}}_1 + {}^{B}\ddot{\mathbf{r}}_2 + {}^{B}\ddot{\mathbf{r}}_3 \right) \quad (28) $$

This leaves the components of the angular acceleration as the remaining system unknowns. In the original work [9], the authors used a minimization of least squares error approach based on the error vector [?]. The form of the objective function for such an approach is [?]^T**C**[?], where **C** is the variance-covariance matrix. If the assumption is made that the errors are uncorrelated, **C** reduces to the identity matrix and the objective function reduces to a scalar. If the error terms are renumbered from one to nine (the first three terms associated with the first sensor block, the second three terms associated with the second sensor block and the last three terms associated with the third sensor block) then the following holds:

$$ \left[\boldsymbol{\varepsilon} \right]^T \mathbf{C} \left[\boldsymbol{\varepsilon} \right] = \left[\boldsymbol{\varepsilon} \right]^T \mathbf{I} \left[\boldsymbol{\varepsilon} \right] = \left[\boldsymbol{\varepsilon} \right]^T \left[\boldsymbol{\varepsilon} \right] = \varepsilon_i \varepsilon_i = \sum_{i=1}^{9} \varepsilon_i^{\,2} \quad (29) $$

The objective function is minimized when the partial derivatives of the function, with respect to the system variables, are zero valued.

$$ \frac{\partial}{\partial \left({}^{B}_{G}\dot{\boldsymbol{\omega}}_B \right)} \left(\left[\boldsymbol{\varepsilon} \right]^T \left[\boldsymbol{\varepsilon} \right] \right) = \frac{\partial \left(\left[\boldsymbol{\varepsilon} \right]^T \right)}{\partial \left({}^{B}_{G}\dot{\boldsymbol{\omega}}_B \right)} \left[\boldsymbol{\varepsilon} \right] + \left[\boldsymbol{\varepsilon} \right]^T \frac{\partial \left[\boldsymbol{\varepsilon} \right]}{\partial \left({}^{B}_{G}\dot{\boldsymbol{\omega}}_B \right)} = \mathbf{0} \quad (30) $$

Equation (30) can be rewritten, by noting the following (using indexed notation):

$$ \begin{aligned} \frac{\partial}{\partial \left({}^{B}_{G}\dot{\boldsymbol{\omega}}_B \right)} \left(\left[\boldsymbol{\varepsilon} \right]^T \left[\boldsymbol{\varepsilon} \right] \right) &= \frac{\partial \varepsilon_i \varepsilon_i}{\partial {}^{B}_{G}\dot{\omega}_{B-j}} \\ &= \frac{\partial \varepsilon_i \varepsilon_i}{\partial {}^{B}_{G}\dot{\omega}_{B-j}} \varepsilon_i + \varepsilon_i \frac{\partial \varepsilon_i}{\partial {}^{B}_{G}\dot{\omega}_{B-j}} \\ &= 2 \frac{\partial \varepsilon_i}{\partial {}^{B}_{G}\dot{\omega}_{B-j}} \varepsilon_i = 2 \frac{\partial \left(\left[\boldsymbol{\varepsilon} \right]^T \right)}{\partial \left({}^{B}_{G}\dot{\boldsymbol{\omega}}_B \right)} \left[\boldsymbol{\varepsilon} \right] \end{aligned} \quad (31) $$

The partial derivative of the transpose of the error vector, with respect to the angular acceleration vector, is:

$$ \frac{\partial \left(\boldsymbol{\varepsilon}^T \right)}{\partial \left({}^{B}_{G}\dot{\boldsymbol{\omega}}_B \right)} = -\left[{}^{B}\tilde{\mathbf{r}} \right]^T \quad (32) $$

Substitution of this result and the result from equation (22) into equation (31) results in the following:

$$ -\left[{}^{B}\tilde{\mathbf{r}} \right]^T \left[{}^{B}_{G}\ddot{\mathbf{r}}_o \right] + \left[{}^{B}\tilde{\mathbf{r}} \right]^T \left[{}^{B}\tilde{\mathbf{r}} \right] {}^{B}_{G}\dot{\boldsymbol{\omega}}_B - \left[{}^{B}\tilde{\mathbf{r}} \right]^T \left[{}^{B}\boldsymbol{\upsilon} \right] = \mathbf{0} \quad (33) $$

Expanding the first term in equation (33):

$$\left[{}^{B}\tilde{\mathbf{r}}\right]^{T}\left[{}^{B}_{G}\ddot{\mathbf{r}}_{o}\right]=\begin{bmatrix} {}^{B}_{G}\ddot{\mathbf{r}}_{o2}\left({}^{B}\mathbf{r}_{13}+{}^{B}\mathbf{r}_{23}+{}^{B}\mathbf{r}_{33}\right)- \\ {}^{B}_{G}\ddot{\mathbf{r}}_{o3}\left({}^{B}\mathbf{r}_{12}+{}^{B}\mathbf{r}_{22}+{}^{B}\mathbf{r}_{32}\right) \\ {}^{B}_{G}\ddot{\mathbf{r}}_{o3}\left({}^{B}\mathbf{r}_{11}+{}^{B}\mathbf{r}_{21}+{}^{B}\mathbf{r}_{31}\right)- \\ {}^{B}_{G}\ddot{\mathbf{r}}_{o1}\left({}^{B}\mathbf{r}_{13}+{}^{B}\mathbf{r}_{23}+{}^{B}\mathbf{r}_{33}\right) \\ {}^{B}_{G}\ddot{\mathbf{r}}_{o1}\left({}^{B}\mathbf{r}_{12}+{}^{B}\mathbf{r}_{22}+{}^{B}\mathbf{r}_{32}\right)- \\ {}^{B}_{G}\ddot{\mathbf{r}}_{o2}\left({}^{B}\mathbf{r}_{11}+{}^{B}\mathbf{r}_{21}+{}^{B}\mathbf{r}_{31}\right) \end{bmatrix} \tag{34}$$

From equation (27) it can readily be seen that each of the parenthetical terms in equation (34) is zero-valued. As a result, the entirety of this term is zero-valued. Equation (33) can then be rewritten as:

$$\left[{}^{B}\tilde{\mathbf{r}}\right]^{T}\left[{}^{B}\tilde{\mathbf{r}}\right]{}^{B}_{G}\dot{\boldsymbol{\omega}}_{B}-\left[{}^{B}\tilde{\mathbf{r}}\right]^{T}\left[{}^{B}\boldsymbol{\upsilon}\right]=\mathbf{0} \tag{35}$$

Solving this equation for the angular acceleration:

$${}^{B}_{G}\dot{\boldsymbol{\omega}}_{B}=\left(\left[{}^{B}\tilde{\mathbf{r}}\right]^{T}\left[{}^{B}\tilde{\mathbf{r}}\right]\right)^{-1}\left[{}^{B}\tilde{\mathbf{r}}\right]^{T}\left[{}^{B}\boldsymbol{\upsilon}\right] \tag{36}$$

2.4 Extension of the original solution

The original work [9] can readily be extended, using the same general methodological approach, but with the elimination of the assumption that the center of mass of the body lies at the geometric centroid of the (triangular) plane defined by the three sensor block body frame locations. The system unknowns then consist of the three components of the center of mass body frame expressed translational acceleration and the three components of the angular acceleration. It is useful to present the solution steps with the vectors expanded.

$$\begin{aligned}\varepsilon_1=&-{}^{B}_{G}\ddot{r}_{11}+{}^{B}_{G}\ddot{r}_{o1}+{}^{B}r_{13}\,{}^{B}_{G}\dot{\omega}_{B-2}-{}^{B}r_{12}\,{}^{B}_{G}\dot{\omega}_{B-3}\\&-{}^{B}r_{11}\,{}^{B}_{G}\omega_{B-2}{}^{2}-{}^{B}r_{11}\,{}^{B}_{G}\omega_{B-3}{}^{2}+{}^{B}r_{12}\,{}^{B}_{G}\omega_{B-1}\,{}^{B}_{G}\omega_{B-2}\\&+{}^{B}r_{13}\,{}^{B}_{G}\omega_{B-1}\,{}^{B}_{G}\omega_{B-3}\end{aligned} \tag{37}$$

$$\begin{aligned}\varepsilon_2=&-{}^{B}_{G}\ddot{r}_{21}+{}^{B}_{G}\ddot{r}_{o1}+{}^{B}r_{23}\,{}^{B}_{G}\dot{\omega}_{B-2}-{}^{B}r_{22}\,{}^{B}_{G}\dot{\omega}_{B-3}\\&-{}^{B}r_{21}\,{}^{B}_{G}\omega_{B-2}{}^{2}-{}^{B}r_{21}\,{}^{B}_{G}\omega_{B-3}{}^{2}+{}^{B}r_{22}\,{}^{B}_{G}\omega_{B-1}\,{}^{B}_{G}\omega_{B-2}\\&+{}^{B}r_{23}\,{}^{B}_{G}\omega_{B-1}\,{}^{B}_{G}\omega_{B-3}\end{aligned} \tag{38}$$

$$\begin{aligned}\varepsilon_3=&-{}^{B}_{G}\ddot{r}_{31}+{}^{B}_{G}\ddot{r}_{o1}+{}^{B}r_{33}\,{}^{B}_{G}\dot{\omega}_{B-2}-{}^{B}r_{32}\,{}^{B}_{G}\dot{\omega}_{B-3}\\&-{}^{B}r_{31}\,{}^{B}_{G}\omega_{B-2}{}^{2}-{}^{B}r_{31}\,{}^{B}_{G}\omega_{B-3}{}^{2}+{}^{B}r_{32}\,{}^{B}_{G}\omega_{B-1}\,{}^{B}_{G}\omega_{B-2}\\&+{}^{B}r_{33}\,{}^{B}_{G}\omega_{B-1}\,{}^{B}_{G}\omega_{B-3}\end{aligned} \tag{39}$$

$$\begin{aligned}\varepsilon_4=&-{}^{B}_{G}\ddot{r}_{12}+{}^{B}_{G}\ddot{r}_{o2}+{}^{B}r_{11}\,{}^{B}_{G}\dot{\omega}_{B-3}-{}^{B}r_{13}\,{}^{B}_{G}\dot{\omega}_{B-1}\\&-{}^{B}r_{12}\,{}^{B}_{G}\omega_{B-1}{}^{2}-{}^{B}r_{12}\,{}^{B}_{G}\omega_{B-3}{}^{2}+{}^{B}r_{11}\,{}^{B}_{G}\omega_{B-1}\,{}^{B}_{G}\omega_{B-2}\\&+{}^{B}r_{13}\,{}^{B}_{G}\omega_{B-2}\,{}^{B}_{G}\omega_{B-3}\end{aligned} \tag{40}$$

$$\begin{aligned}\varepsilon_5=&-{}^{B}_{G}\ddot{r}_{22}+{}^{B}_{G}\ddot{r}_{o2}+{}^{B}r_{21}\,{}^{B}_{G}\dot{\omega}_{B-3}-{}^{B}r_{23}\,{}^{B}_{G}\dot{\omega}_{B-1}\\&-{}^{B}r_{22}\,{}^{B}_{G}\omega_{B-1}{}^{2}-{}^{B}r_{22}\,{}^{B}_{G}\omega_{B-3}{}^{2}+{}^{B}r_{21}\,{}^{B}_{G}\omega_{B-1}\,{}^{B}_{G}\omega_{B-2}\\&+{}^{B}r_{23}\,{}^{B}_{G}\omega_{B-2}\,{}^{B}_{G}\omega_{B-3}\end{aligned} \tag{41}$$

$$\begin{aligned}\varepsilon_6=&-{}^{B}_{G}\ddot{r}_{32}+{}^{B}_{G}\ddot{r}_{o2}+{}^{B}r_{31}\,{}^{B}_{G}\dot{\omega}_{B-3}-{}^{B}r_{33}\,{}^{B}_{G}\dot{\omega}_{B-1}\\&-{}^{B}r_{32}\,{}^{B}_{G}\omega_{B-1}{}^{2}-{}^{B}r_{32}\,{}^{B}_{G}\omega_{B-3}{}^{2}+{}^{B}r_{31}\,{}^{B}_{G}\omega_{B-1}\,{}^{B}_{G}\omega_{B-2}\\&+{}^{B}r_{33}\,{}^{B}_{G}\omega_{B-2}\,{}^{B}_{G}\omega_{B-3}\end{aligned} \tag{42}$$

$$\begin{aligned}\varepsilon_7=&-{}^{B}_{G}\ddot{r}_{13}+{}^{B}_{G}\ddot{r}_{o3}+{}^{B}r_{12}\,{}^{B}_{G}\dot{\omega}_{B-1}-{}^{B}r_{11}\,{}^{B}_{G}\dot{\omega}_{B-2}\\&-{}^{B}r_{13}\,{}^{B}_{G}\omega_{B-1}{}^{2}-{}^{B}r_{13}\,{}^{B}_{G}\omega_{B-2}{}^{2}+{}^{B}r_{11}\,{}^{B}_{G}\omega_{B-1}\,{}^{B}_{G}\omega_{B-3}\\&+{}^{B}r_{12}\,{}^{B}_{G}\omega_{B-2}\,{}^{B}_{G}\omega_{B-3}\end{aligned} \tag{43}$$

$$\begin{aligned}\varepsilon_8=&-{}^{B}_{G}\ddot{r}_{23}+{}^{B}_{G}\ddot{r}_{o3}+{}^{B}r_{22}\,{}^{B}_{G}\dot{\omega}_{B-1}-{}^{B}r_{21}\,{}^{B}_{G}\dot{\omega}_{B-2}\\&-{}^{B}r_{23}\,{}^{B}_{G}\omega_{B-1}{}^{2}-{}^{B}r_{23}\,{}^{B}_{G}\omega_{B-2}{}^{2}+{}^{B}r_{21}\,{}^{B}_{G}\omega_{B-1}\,{}^{B}_{G}\omega_{B-3}\\&+{}^{B}r_{22}\,{}^{B}_{G}\omega_{B-2}\,{}^{B}_{G}\omega_{B-3}\end{aligned} \tag{44}$$

$$\begin{aligned}\varepsilon_9=&-{}^{B}_{G}\ddot{r}_{33}+{}^{B}_{G}\ddot{r}_{o3}+{}^{B}r_{32}\,{}^{B}_{G}\dot{\omega}_{B-1}-{}^{B}r_{31}\,{}^{B}_{G}\dot{\omega}_{B-2}\\&-{}^{B}r_{33}\,{}^{B}_{G}\omega_{B-1}{}^{2}-{}^{B}r_{33}\,{}^{B}_{G}\omega_{B-2}{}^{2}+{}^{B}r_{31}\,{}^{B}_{G}\omega_{B-1}\,{}^{B}_{G}\omega_{B-3}\\&+{}^{B}r_{32}\,{}^{B}_{G}\omega_{B-2}\,{}^{B}_{G}\omega_{B-3}\end{aligned} \tag{45}$$

The scaler $[\square]^{T}C[\square]=[\square]^{T}I[\square]=[\square]^{T}[\square]$ can be generated by squaring each of the nine equations from (37) to (45) and summing the results. To simplify the presentation for this section, the following nomenclature simplifications are used:

$$\begin{aligned}{}^{B}r_{ij}&\rightarrow r_{ij} & {}^{B}_{G}\ddot{r}_{ij}&\rightarrow \ddot{r}_{ij}\\ {}^{B}_{G}\omega_{B-i}&\rightarrow \omega_{i} & {}^{B}_{G}\dot{\omega}_{B-i}&\rightarrow \dot{\omega}_{i}\end{aligned} \tag{46}$$

The six partial derivatives of the sum of square errors are comprised of the three partial derivatives with respect to each component of the body frame expressed translational acceleration of **o** and the three partial derivatives of each component of the body frame expressed angular acceleration vector of the body frame about the inertial frame.

$$\frac{\partial}{\partial \ddot{r}_{o1}}\left(\left[\boldsymbol{\varepsilon}\right]^{T}\left[\boldsymbol{\varepsilon}\right]\right)= 2\begin{pmatrix} 3\ddot{r}_{o1}-\sum_{i=1}^{3}\ddot{r}_{i1}+\dot{\omega}_{2}\sum_{i=1}^{3}r_{i3}-\dot{\omega}_{3}\sum_{i=1}^{3}r_{i2}- \\ \left(\omega_{2}{}^{2}+\omega_{3}{}^{2}\right)\sum_{i=1}^{3}r_{i1}+\omega_{1}\omega_{2}\sum_{i=1}^{3}r_{i2}+\omega_{1}\omega_{3}\sum_{i=1}^{3}r_{i3} \end{pmatrix} \tag{47}$$

$$\frac{\partial}{\partial \ddot{r}_{o2}}\left(\left[\boldsymbol{\varepsilon}\right]^{T}\left[\boldsymbol{\varepsilon}\right]\right)= 2\begin{pmatrix} 3\ddot{r}_{o2}-\sum_{i=1}^{3}\ddot{r}_{i2}+\dot{\omega}_{3}\sum_{i=1}^{3}r_{i1}-\dot{\omega}_{1}\sum_{i=1}^{3}r_{i3}- \\ \left(\omega_{1}{}^{2}+\omega_{3}{}^{2}\right)\sum_{i=1}^{3}r_{i2}+\omega_{1}\omega_{2}\sum_{i=1}^{3}r_{i1}+\omega_{2}\omega_{3}\sum_{i=1}^{3}r_{i3} \end{pmatrix} \tag{48}$$

$$\frac{\partial}{\partial \ddot{r}_{o3}}\left([\varepsilon]^T[\varepsilon]\right)=$$

$$2\begin{pmatrix} 3\ddot{r}_{o3}-\sum_{i=1}^{3}\ddot{r}_{i3}+\dot{\omega}_1\sum_{i=1}^{3}r_{i2}-\dot{\omega}_2\sum_{i=1}^{3}r_{i1}- \\ \left(\omega_1^{\,2}+\omega_2^{\,2}\right)\sum_{i=1}^{3}r_{i3}+\omega_1\omega_3\sum_{i=1}^{3}r_{i1}+\omega_2\omega_3\sum_{i=1}^{3}r_{i2} \end{pmatrix} \quad (49)$$

$$\frac{\partial}{\partial \dot{\omega}_1}\left([\varepsilon]^T[\varepsilon]\right)=$$

$$2\begin{pmatrix} -\left(\sum_{i=1}^{3}r_{i3}\right)\ddot{r}_{o2}+\left(\sum_{i=1}^{3}r_{i2}\right)\ddot{r}_{o3}+\sum_{i=1}^{3}\left(r_{i3}\ddot{r}_{i2}-r_{i2}\ddot{r}_{i3}\right) \\ +\left(\sum_{i=1}^{3}\left(r_{i2}^{\,2}+r_{13}^{\,2}\right)\right)\dot{\omega}_1 \\ -\left(\sum_{i=1}^{3}r_{i1}r_{i2}\right)\dot{\omega}_2-\left(\sum_{i=1}^{3}r_{i1}r_{i3}\right)\dot{\omega}_3 \\ +\left(\sum_{i=1}^{3}r_{i2}r_{i3}\right)\left(\omega_3^{\,2}-\omega_2^{\,2}\right)-\left(\sum_{i=1}^{3}r_{i1}r_{i3}\right)\omega_1\omega_2 \\ +\left(\sum_{i=1}^{3}r_{i1}r_{i2}\right)\omega_1\omega_3+\left(\sum_{i=1}^{3}\left(r_{i2}^{\,2}-r_{13}^{\,2}\right)\right)\omega_2\omega_3 \end{pmatrix} \quad (50)$$

$$\frac{\partial}{\partial \dot{\omega}_2}\left([\varepsilon]^T[\varepsilon]\right)=$$

$$2\begin{pmatrix} +\left(\sum_{i=1}^{3}r_{i3}\right)\ddot{r}_{o1}-\left(\sum_{i=1}^{3}r_{i1}\right)\ddot{r}_{o3}+\sum_{i=1}^{3}\left(r_{i1}\ddot{r}_{i3}-r_{i3}\ddot{r}_{i1}\right) \\ -\left(\sum_{i=1}^{3}r_{i1}r_{i2}\right)\dot{\omega}_1+\left(\sum_{i=}^{3}\left(r_{i1}^{\,2}+r_{i3}^{\,2}\right)\right)\dot{\omega}_2 \\ -\left(\sum_{i=1}^{3}r_{i2}r_{i3}\right)\dot{\omega}_3+\left(\sum_{i=1}^{3}r_{i1}r_{i3}\right)\left(\omega_1^{\,2}-\omega_3^{\,2}\right) \\ +\left(\sum_{i=1}^{3}r_{i2}r_{i3}\right)\omega_1\omega_2+\left(\sum_{i=1}^{3}\left(r_{i3}^{\,2}-r_{i1}^{\,2}\right)\right)\omega_1\omega_3 \\ -\left(\sum_{i=1}^{3}r_{i1}r_{i2}\right)\omega_2\omega_3 \end{pmatrix} \quad (51)$$

$$\frac{\partial}{\partial \dot{\omega}_3}\left([\varepsilon]^T[\varepsilon]\right)=$$

$$2\begin{pmatrix} -\left(\sum_{i=1}^{3}r_{i2}\right)\ddot{r}_{o1}+\left(\sum_{i=1}^{3}r_{i1}\right)\ddot{r}_{o2}+\sum_{i=1}^{3}\left(r_{i2}\ddot{r}_{i1}-r_{i1}\ddot{r}_{i2}\right) \\ -\left(\sum_{i=1}^{3}r_{i1}r_{i3}\right)\dot{\omega}_1-\left(\sum_{i=1}^{3}r_{i2}r_{i3}\right)\dot{\omega}_2 \\ +\left(\sum_{i=1}^{3}\left(r_{i1}^{\,2}+r_{i2}^{\,2}\right)\right)\dot{\omega}_3 \\ +\left(\sum_{i=1}^{3}r_{i1}r_{i2}\right)\left(\omega_2^{\,2}-\omega_1^{\,2}\right)+\left(\sum_{i=1}^{3}\left(r_{i1}^{\,2}-r_{i2}^{\,2}\right)\right)\omega_1\omega_2 \\ -\left(\sum_{i=1}^{3}r_{i2}r_{i3}\right)\omega_1\omega_3+\left(\sum_{i=1}^{3}r_{i1}r_{i3}\right)\omega_2\omega_3 \end{pmatrix} \quad (52)$$

These six equations can be placed into the following compact vector-matrix form.

$$[\rho]\,{}^{B}\mathbf{y}={}^{B}\mathbf{C} \quad (53)$$

The term [⍰] is a 6 x 6 matrix. The first row of this matrix is:

$$[\rho]_1=\begin{bmatrix} 3 & 0 & 0 & \cdots \\ \cdots & 0 & +\sum_{i=1}^{3}r_{i3} & -\sum_{i=1}^{3}r_{i2} \end{bmatrix} \quad (54)$$

The second row of this matrix is:

$$[\rho]_2=\begin{bmatrix} 0 & 3 & 0 & \cdots \\ \cdots & -\sum_{i=1}^{3}r_{i3} & 0 & +\sum_{i=1}^{3}r_{i1} \end{bmatrix} \quad (55)$$

The third row of this matrix is:

$$[\rho]_3=\begin{bmatrix} 0 & 0 & 3 & \cdots \\ \cdots & +\sum_{i=1}^{3}r_{i2} & -\sum_{i=1}^{3}r_{i1} & 0 \end{bmatrix} \quad (56)$$

The fourth row of this matrix is:

$$[\rho]_4=\begin{bmatrix} 0 & -\sum_{i=1}^{3}r_{i3} & \cdots \\ \cdots & +\sum_{i=1}^{3}r_{i2} & +\sum_{i=1}^{3}\left(r_{i2}^{\,2}+r_{i3}^{\,2}\right) & \cdots \\ \cdots & -\sum_{i=1}^{3}r_{i1}r_{i2} & -\sum_{i=1}^{3}r_{i1}r_{i3} \end{bmatrix} \quad (57)$$

The fifth row of this matrix is:

$$[\rho]_5=\begin{bmatrix} +\sum_{i=1}^{3}r_{i3} & 0 & \cdots \\ \cdots & -\sum_{i=1}^{3}r_{i1} & -\sum_{i=1}^{3}r_{i1}r_{i2} & \cdots \\ \cdots & +\sum_{i=1}^{3}\left(r_{i1}^{\,2}+r_{i3}^{\,2}\right) & -\sum_{i=1}^{3}r_{i2}r_{i3} \end{bmatrix} \quad (58)$$

The last row of this matrix is:

$$[\rho]_6=\begin{bmatrix} -\sum_{i=1}^{3}r_{i2} & +\sum_{i=1}^{3}r_{i1} & \cdots \\ \cdots & 0 & -\sum_{i=1}^{3}r_{i1}r_{i3} & \cdots \\ \cdots & -\sum_{i=1}^{3}r_{i2}r_{i3} & +\sum_{i=1}^{3}\left(r_{i1}^{\,2}+r_{i2}^{\,2}\right) \end{bmatrix} \quad (59)$$

The vector ${}^{B}\mathbf{y}$ is the 6 x 1 column vector of system unknowns.

$${}^{B}\mathbf{y}=\begin{bmatrix}\ddot{r}_{o1} & \ddot{r}_{o2} & \ddot{r}_{o3} & \dot{\omega}_1 & \dot{\omega}_2 & \dot{\omega}_3\end{bmatrix}^T \quad (60)$$

Finally, ${}^{B}\mathbf{C}$ is a 6 x 1 column vector containing the terms associated with the measured peripheral acceleration and the quadratic angular velocity terms. The first row is:

$$\left[{}^{B}C\right]_1 = \sum_{i=1}^{3}\ddot{r}_{i1} + \left(\sum_{i=1}^{3} r_{i1}\right)\left(\omega_2{}^2 + \omega_3{}^2\right) - \left(\sum_{i=1}^{3} r_{i2}\right)\omega_1\omega_2 - \left(\sum_{i=1}^{3} r_{i3}\right)\omega_1\omega_3 \quad (61)$$

The second row is:

$$\left[{}^{B}C\right]_2 = \sum_{i=1}^{3}\ddot{r}_{i2} + \left(\sum_{i=1}^{3} r_{i2}\right)\left(\omega_1{}^2 + \omega_3{}^2\right) - \left(\sum_{i=1}^{3} r_{i1}\right)\omega_1\omega_2 - \left(\sum_{i=1}^{3} r_{i3}\right)\omega_2\omega_3 \quad (62)$$

The third row is:

$$\left[{}^{B}C\right]_3 = \sum_{i=1}^{3}\ddot{r}_{i3} + \left(\sum_{i=1}^{3} r_{i3}\right)\left(\omega_1{}^2 + \omega_2{}^2\right) - \left(\sum_{i=1}^{3} r_{i1}\right)\omega_1\omega_2 - \left(\sum_{i=1}^{3} r_{i2}\right)\omega_2\omega_3 \quad (63)$$

The fourth row is:

$$\left[{}^{B}C\right]_4 = -\sum_{i=1}^{3} r_{i3}\ddot{r}_{i2} + \sum_{i=1}^{3} r_{i2}\ddot{r}_{i3} - \left(\sum_{i=1}^{3} r_{i2}r_{i3}\right)\left(\omega_3{}^2 - \omega_2{}^2\right) + \left(\sum_{i=1}^{3} r_{i1}r_{i3}\right)\omega_1\omega_2 - \left(\sum_{i=1}^{3} r_{i1}r_{i2}\right)\omega_1\omega_3 - \left(\sum_{i=1}^{3}\left(r_{i2}{}^2 - r_{i3}{}^2\right)\right)\omega_2\omega_3 \quad (64)$$

The fifth row is:

$$\left[{}^{B}C\right]_5 = -\sum_{i=1}^{3} r_{i1}\ddot{r}_{i3} + \sum_{i=1}^{3} r_{i3}\ddot{r}_{i1} - \left(\sum_{i=1}^{3} r_{i1}r_{i3}\right)\left(\omega_1{}^2 - \omega_3{}^2\right) - \left(\sum_{i=1}^{3} r_{i2}r_{i3}\right)\omega_1\omega_2 - \left(\sum_{i=1}^{3}\left(r_{i3}{}^2 - r_{i1}{}^2\right)\right)\omega_1\omega_3 + \left(\sum_{i=1}^{3} r_{i1}r_{i2}\right)\omega_2\omega_3 \quad (65)$$

The final row is:

$$\left[{}^{B}C\right]_6 = -\sum_{i=1}^{3} r_{i2}\ddot{r}_{i1} + \sum_{i=1}^{3} r_{i1}\ddot{r}_{i2} - \left(\sum_{i=1}^{3} r_{i1}r_{i2}\right)\left(\omega_2{}^2 - \omega_1{}^2\right) - \left(\sum_{i=1}^{3}\left(r_{i1}{}^2 - r_{i2}{}^2\right)\right)\omega_1\omega_2 + \left(\sum_{i=1}^{3} r_{i2}r_{i3}\right)\omega_1\omega_3 - \left(\sum_{i=1}^{3} r_{i1}r_{i3}\right)\omega_2\omega_3 \quad (66)$$

When [⍰] is non-singular (i.e. det[⍰] ≠ 0), equation (53) can be inverted to solve for ${}^{B}\mathbf{y}$.

$${}^{B}\mathbf{y} = \left[\rho\right]^{-1}{}^{B}\mathbf{C} \quad (67)$$

2.5 Gravitational acceleration and specific force

The inertial frame expression for the peripheral point translational acceleration, was given by equation (16). This acceleration can also be written as:

$${}^{G}\ddot{\mathbf{r}}_k = {}^{G}\mathbf{f}_k + {}^{G}\mathbf{g} \quad (68)$$

Where ${}^{G}\mathbf{f}_k$ is the inertial frame expression of the specific force at $\mathbf{p}_k$ and ${}^{G}\mathbf{g}$ is the inertial frame expression of the acceleration due to gravity. For each sensor block, we may define a vector in which one element, corresponding with the sensing axis under consideration, has unity value and with the other two elements being zero valued.

$$\left({}^{B}\mathbf{s}_k\right)^{T} = \begin{bmatrix} s_{k1} & s_{k2} & s_{k3} \end{bmatrix} \quad (69)$$

The accelerometer output at $\mathbf{p}_k$ can then be expressed as:

$${}^{B}_{G}\ddot{\mathbf{r}}_k = \left({}^{B}\mathbf{s}_k\right)^{T}{}^{B}\mathbf{f}_k = \left({}^{B}\mathbf{s}_k\right)^{T}{}^{B}R_G\,{}^{G}\mathbf{f}_k \quad (70)$$

Solving equation (68) for ${}^{G}\mathbf{f}_k$ and substituting the result into equation (70):

$${}^{B}_{G}\ddot{\mathbf{r}}_k = \left({}^{B}\mathbf{s}_k\right)^{T}{}^{B}R_G\left({}^{G}\ddot{\mathbf{r}}_k - {}^{G}\mathbf{g}\right) \quad (71)$$

Substituting for the inertial frame acceleration at $\mathbf{p}_k$ from equation (16):

$${}^{B}_{G}\ddot{\mathbf{r}}_k = \left({}^{B}\mathbf{s}_k\right)^{T}{}^{B}R_G\left({}^{G}\ddot{\mathbf{r}}_o - {}^{G}\mathbf{g}\right) + \left({}^{B}\mathbf{s}_k\right)^{T}\left({}^{B}_{G}\dot{\boldsymbol{\omega}}_B \times {}^{B}\mathbf{r}_k\right) + \left({}^{B}\mathbf{s}_k\right)^{T}\left({}^{B}_{G}\boldsymbol{\omega}_B \times \left({}^{B}_{G}\boldsymbol{\omega}_B \times {}^{B}\mathbf{r}_k\right)\right) \quad (72)$$

The term in the first parenthetical on the right side of the equality is simply the inertial frame expression of the specific force at **o**. When premultiplied by the DCM ${}^{B}R_G$, as shown in the equation, it becomes the body frame expression of the same.

$${}^{B}_{G}\ddot{\mathbf{r}}_k = \left({}^{B}\mathbf{s}_k\right)^{T}{}^{B}\mathbf{f}_o + \left({}^{B}\mathbf{s}_k\right)^{T}\left({}^{B}_{G}\dot{\boldsymbol{\omega}}_B \times {}^{B}\mathbf{r}_k\right) + \left({}^{B}\mathbf{s}_k\right)^{T}\left({}^{B}_{G}\boldsymbol{\omega}_B \times \left({}^{B}_{G}\boldsymbol{\omega}_B \times {}^{B}\mathbf{r}_k\right)\right) \quad (73)$$

When the number of individual sensors is greater than or equal to 12, depending upon senor arrangement, the vector-matrix equation using equation (73) as a basis can be solved algebraically for the specific force at **o**, the angular acceleration and the quadratic angular velocity [21]. It is instructive to derive this solution. The vector-matrix form obtained after writing equation (73) for each sensing axis and collecting the results is:

$$\left[{}^{B}\ddot{\mathbf{r}}_k\right] = \mathbf{J}\mathbf{y} \quad (74)$$

Here, $\left[{}^{B}\ddot{\mathbf{r}}_{k}\right]$ is the column vector with each row containing the readings for a single sensor axis. The vector is of order n x 1{n: n ≥ 12}. The term J, known as the configuration matrix, is of order n x 12. The first three columns of the k^{th} row of the matrix are:

$$J_{k,1-3}=\begin{bmatrix}{}^{B}s_{k1} & {}^{B}s_{k2} & {}^{B}s_{k3}\end{bmatrix} \tag{75}$$

Columns four through six of the k^{th} row of the matrix are:

$$J_{k,4-6}=\begin{bmatrix}{}^{B}s_{k3}\,{}^{B}r_{k2}-{}^{B}s_{k2}\,{}^{B}r_{k3} & {}^{B}s_{k1}\,{}^{B}r_{k3}-{}^{B}s_{k3}\,{}^{B}r_{k1} & \cdots\\ \cdots & {}^{B}s_{k2}\,{}^{B}r_{k1}-{}^{B}s_{k1}\,{}^{B}r_{k2} & \end{bmatrix} \tag{76}$$

Columns seven through nine of the k^{th} row of the matrix are:

$$J_{k,7-9}=\begin{bmatrix}-{}^{B}s_{k2}\,{}^{B}r_{k2}-{}^{B}s_{k3}\,{}^{B}r_{k3} & -{}^{B}s_{k1}\,{}^{B}r_{k1}-{}^{B}s_{k3}\,{}^{B}r_{k3} & \cdots\\ \cdots & -{}^{B}s_{k1}\,{}^{B}r_{k1}-{}^{B}s_{k2}\,{}^{B}r_{k2} & \end{bmatrix} \tag{77}$$

Columns ten through twelve of the k^{th} row of the matrix are:

$$J_{k,10-12}=\begin{bmatrix}{}^{B}s_{k1}\,{}^{B}r_{k2}+{}^{B}s_{k2}\,{}^{B}r_{k1} & {}^{B}s_{k1}\,{}^{B}r_{k3}+{}^{B}s_{k3}\,{}^{B}r_{k1} & \cdots\\ \cdots & {}^{B}s_{k2}\,{}^{B}r_{k3}+{}^{B}s_{k3}\,{}^{B}r_{k2} & \end{bmatrix} \tag{78}$$

The vector **y** is the 12 x 1 column vector of system unknowns. Using the simplified terminology shown by equation (46) and using ${}^{B}f_{oi} \rightarrow f_{oi}$, the first six rows of **y** are:

$$\mathbf{y}_{1-6}=\begin{bmatrix}f_{o1} & f_{o2} & f_{o3} & \dot{\omega}_{1} & \dot{\omega}_{2} & \dot{\omega}_{3}\end{bmatrix}^{T} \tag{79}$$

The last six rows of **y** are:

$$\mathbf{y}_{7-12}=\begin{bmatrix}\omega_{1}^{2} & \omega_{2}^{2} & \omega_{3}^{2} & \omega_{1}\omega_{2} & \omega_{1}\omega_{3} & \omega_{2}\omega_{3}\end{bmatrix}^{T} \tag{80}$$

When the number of uniaxial sensors is equal to 12, J is a square matrix. If the matrix is non-singular, the unknowns can be solved for by inverting equation (74).

$$\mathbf{y}=J^{-1}\left[{}^{B}\ddot{\mathbf{r}}_{k}\right] \tag{81}$$

When the number of uniaxial sensors exceeds 12, J is no longer a square matrix. In such cases, the left matrix inverse may be used. This is defined as:

$$J^{+}=\left(J^{T}J\right)^{-1}J^{T} \tag{82}$$

When the left matrix inverse exists, the solution to equation (74) becomes:

$$\mathbf{y}=J^{+}\left[{}^{B}\ddot{\mathbf{r}}_{k}\right] \tag{83}$$

2.6 Gravity and the standard 3-3-3 approach

For the original approach[9], we return to equation (72) and expand the first term on the right of the equality:

$$\begin{aligned}{}^{B}_{G}\ddot{\mathbf{r}}_{k}&=\left({}^{B}\mathbf{s}_{k}\right)^{T}{}^{B}R_{G}\,{}^{G}\ddot{\mathbf{r}}_{o}-\left({}^{B}\mathbf{s}_{k}\right)^{T}{}^{B}R_{G}\,{}^{G}\mathbf{g}\\&-\left({}^{B}\mathbf{s}_{k}\right)^{T}\left({}^{B}\tilde{\mathbf{r}}_{k}\,{}^{B}_{G}\dot{\boldsymbol{\omega}}_{B}\right)+\left({}^{B}\mathbf{s}_{k}\right)^{T}\left({}^{B}_{G}\tilde{\omega}_{B}\left({}^{B}_{G}\tilde{\omega}_{B}\,{}^{B}\mathbf{r}_{k}\right)\right)\end{aligned} \tag{84}$$

Evaluating the first term on the right of the equality as before:

$$\begin{aligned}{}^{B}_{G}\ddot{\mathbf{r}}_{k}&=\left({}^{B}\mathbf{s}_{k}\right)^{T}{}^{B}_{G}\ddot{\mathbf{r}}_{o}-\left({}^{B}\mathbf{s}_{k}\right)^{T}{}^{B}R_{G}\,{}^{G}\mathbf{g}\\&-\left({}^{B}\mathbf{s}_{k}\right)^{T}\left({}^{B}\tilde{\mathbf{r}}_{k}\,{}^{B}_{G}\dot{\boldsymbol{\omega}}_{B}\right)+\left({}^{B}\mathbf{s}_{k}\right)^{T}\left({}^{B}_{G}\tilde{\omega}_{B}\left({}^{B}_{G}\tilde{\omega}_{B}\,{}^{B}\mathbf{r}_{k}\right)\right)\end{aligned} \tag{85}$$

The kth row in the error vector, before renumbering, becomes:

$$\begin{aligned}\boldsymbol{\varepsilon}_{k}&=\left({}^{B}\mathbf{s}_{k}\right)^{T}{}^{B}_{G}\ddot{\mathbf{r}}_{o}-\left({}^{B}\mathbf{s}_{k}\right)^{T}\left({}^{B}\tilde{\mathbf{r}}_{k}\,{}^{B}_{G}\dot{\boldsymbol{\omega}}_{B}\right)\\&+\left({}^{B}\mathbf{s}_{k}\right)^{T}\left({}^{B}_{G}\tilde{\omega}_{B}\left({}^{B}_{G}\tilde{\omega}_{B}\,{}^{B}\mathbf{r}_{k}\right)\right)-{}^{B}_{G}\ddot{\mathbf{r}}_{k}-\left({}^{B}\mathbf{s}_{k}\right)^{T}{}^{B}R_{G}\,{}^{G}\mathbf{g}\end{aligned} \tag{86}$$

Following the previous approach:

$$\left[\boldsymbol{\varepsilon}\right]=\left[{}^{B}\mathbf{s}\right]^{T}\left[{}^{B}_{G}\ddot{\mathbf{r}}_{o}\right]-\left[{}^{B}\mathbf{s}\right]^{T}\left[{}^{B}\tilde{\mathbf{r}}\right]\left({}^{B}_{G}\dot{\boldsymbol{\omega}}_{B}\right)+\left[{}^{B}\boldsymbol{\upsilon}\right] \tag{87}$$

It should be noted that [^{B}?] differs for equation (87), based upon equation (86), when compared to equation (25).

$$\left[{}^{B}\boldsymbol{\upsilon}\right]_{9\times1}=\begin{bmatrix}\left({}^{B}\mathbf{s}_{1}\right)^{T}\left({}^{B}_{G}\tilde{\omega}_{B}\left({}^{B}_{G}\tilde{\omega}_{B}\,{}^{B}\mathbf{r}_{1}\right)\right)-{}^{B}_{G}\ddot{\mathbf{r}}_{1}-\left({}^{B}\mathbf{s}_{1}\right)^{T}{}^{B}R_{G}\,{}^{G}\mathbf{g}\\ \left({}^{B}\mathbf{s}_{2}\right)^{T}\left({}^{B}_{G}\tilde{\omega}_{B}\left({}^{B}_{G}\tilde{\omega}_{B}\,{}^{B}\mathbf{r}_{2}\right)\right)-{}^{B}_{G}\ddot{\mathbf{r}}_{2}-\left({}^{B}\mathbf{s}_{2}\right)^{T}{}^{B}R_{G}\,{}^{G}\mathbf{g}\\ \left({}^{B}\mathbf{s}_{3}\right)^{T}\left({}^{B}_{G}\tilde{\omega}_{B}\left({}^{B}_{G}\tilde{\omega}_{B}\,{}^{B}\mathbf{r}_{3}\right)\right)-{}^{B}_{G}\ddot{\mathbf{r}}_{3}-\left({}^{B}\mathbf{s}_{3}\right)^{T}{}^{B}R_{G}\,{}^{G}\mathbf{g}\end{bmatrix} \tag{88}$$

The translational acceleration, for the original approach, remains unchanged. For the solution for the angular acceleration, the partial derivative of the transpose of the error with respect to the angular acceleration is:

$$\frac{\partial\left(\left[\boldsymbol{\varepsilon}\right]^{T}\right)}{\partial\left({}^{B}_{G}\dot{\boldsymbol{\omega}}_{B}\right)}=-\left(\left[{}^{B}\mathbf{s}\right]^{T}\left[{}^{B}\tilde{\mathbf{r}}\right]\right)^{T} \tag{89}$$

Equation (31), for this case, becomes:

$$\begin{aligned}&2\frac{\partial\left(\left[\boldsymbol{\varepsilon}\right]^{T}\right)}{\partial\left({}^{B}_{G}\dot{\boldsymbol{\omega}}_{B}\right)}\left[\boldsymbol{\varepsilon}\right]=\\&-2\left(\left[{}^{B}\mathbf{s}\right]^{T}\left[{}^{B}\tilde{\mathbf{r}}\right]\right)^{T}\left(\begin{matrix}\left[{}^{B}\mathbf{s}\right]^{T}\left[{}^{B}_{G}\ddot{\mathbf{r}}_{o}\right]-\\ \left[{}^{B}\mathbf{s}\right]^{T}\left[{}^{B}\tilde{\mathbf{r}}\right]\left({}^{B}_{G}\dot{\boldsymbol{\omega}}_{B}\right)+\left[{}^{B}\boldsymbol{\upsilon}\right]\end{matrix}\right)=\mathbf{0}\end{aligned} \tag{90}$$

As a result:

$${}^{B}_{G}\dot{\boldsymbol{\omega}}_{B}=\begin{pmatrix}\left(\left[{}^{B}\mathbf{s}\right]^{T}\left[{}^{B}\tilde{\mathbf{r}}\right]\right)^{T}\cdot\\ \left[{}^{B}\mathbf{s}\right]^{T}\left[{}^{B}\tilde{\mathbf{r}}\right]\end{pmatrix}^{-1}\begin{pmatrix}\left(\left[{}^{B}\mathbf{s}\right]^{T}\left[{}^{B}\tilde{\mathbf{r}}\right]\right)^{T}\left[{}^{B}\mathbf{s}\right]\left[{}^{B}_{G}\ddot{\mathbf{r}}_{o}\right]+\\ \left(\left[{}^{B}\mathbf{s}\right]^{T}\left[{}^{B}\tilde{\mathbf{r}}\right]\right)^{T}\left[{}^{B}\boldsymbol{\upsilon}\right]\end{pmatrix} \tag{91}$$

If the sensing axis vector, given by equation (69), is written for all three sensors that comprise the first instrumentation block:

$$\begin{bmatrix} \left({}^{B}\mathbf{s}_{11}\right)^{T} \\ \left({}^{B}\mathbf{s}_{12}\right)^{T} \\ \left({}^{B}\mathbf{s}_{13}\right)^{T} \end{bmatrix} = \begin{bmatrix} s_{11} & 0 & 0 \\ 0 & s_{12} & 0 \\ 0 & 0 & s_{13} \end{bmatrix} = \begin{bmatrix} 1 & 0 & 0 \\ 0 & 1 & 0 \\ 0 & 0 & 1 \end{bmatrix} = \mathbf{I}_{3\times 3} \qquad (92)$$

When this solution is expanded to system size, $[{}^{B}\mathbf{s}]^{T}$ becomes the 9 x 9 identity matrix $\mathbf{I}_{9x9}$. Equation (91) simplifies to the following:

$$\begin{aligned} {}^{B}_{G}\dot{\boldsymbol{\omega}}_{B} &= \left(\left[{}^{B}\tilde{\mathbf{r}}\right]^{T}\cdot\left[{}^{B}\tilde{\mathbf{r}}\right]\right)^{-1}\left(\left(\left[{}^{B}\tilde{\mathbf{r}}\right]\right)^{T}\left[{}^{B}_{G}\ddot{\mathbf{r}}_{o}\right]+\left[{}^{B}\tilde{\mathbf{r}}\right]^{T}\left[{}^{B}\boldsymbol{\upsilon}\right]\right) \\ &= \left(\left[{}^{B}\tilde{\mathbf{r}}\right]^{T}\cdot\left[{}^{B}\tilde{\mathbf{r}}\right]\right)^{-1}\left(\left[{}^{B}\tilde{\mathbf{r}}\right]^{T}\left[{}^{B}\boldsymbol{\upsilon}\right]\right) \end{aligned} \qquad (93)$$

2.7 Gravity and the expanded 3-3-3 approach

For this case, the DCM ${}^{B}R_{G}$ is simply referenced by its component elements due to the fact that each component element depends upon the manner in which the DCM is parameterized. Therefore, the elements are noted as R with a dual subscript (first subscript referring to the row number and second referring to the column number). Secondly, the inertial frame acceleration due to gravity is defined as:

$${}^{G}\mathbf{g} = \begin{bmatrix} 0 & 0 & -g \end{bmatrix}^{T} \qquad (94)$$

Where g is the magnitude of gravitational acceleration (i.e. g = |1 G| = 9.81 m/sec^2 = 32.2 ft/sec^2). Each of the nine terms that comprise the error vector as shown in equation (86) follow equations (37) through (45) with the following additions: for each of the three error terms associated with the 1-direction, the term $R_{13}g$ is added; for each of the three error terms associated with the 2-direction, the term $R_{23}g$ is added; for each of the three error terms associated with the 3-direction, the term $R_{33}g$ is added. Because these terms are not explicit functions of the center of mass translational acceleration or the angular acceleration, the partial derivatives of the square of the error vector, as shown by equations (47) through (52), are unchanged as is the previously derived solution as per equations (53) through (67).

2.8 Euler-Cardan parameterization

A series of sequential coordinate transformations represented by the DCMs ${}^{2}R_{1}$, ${}^{3}R_{2}$, …, ${}^{n}R_{n-1}$ can readily be represented using a composite DCM.

$${}^{n}R_{1} = {}^{n}R_{n-1}\cdots{}^{3}R_{2}\,{}^{2}R_{1} \qquad (95)$$

The use of a sequential series of three specific rotations is sufficient for defining the relative orientation of a body frame and inertial frame. Twelve distinct sequences exist. Six of these sequences involve an initial rotation about one of the three inertial frame axes. These Euler sequences are typically given with the initial rotation being about one of the inertial frame axes. However, the body frame and inertial frame are typically taken as being coincident prior to the initial rotation and therefore the initial rotation is also taken as being a rotation about the corresponding body frame axis. An Euler sequence differs from a Cardan sequence in that the former involves two rotations about the same body frame axis while the latter does not. In the original work [9], the authors refer to Euler angles in regards to rotational motion but instead use a Cardan sequence. Furthermore, equation (19) of the original reference is incorrect in regards to the first element of the Euler matrix.

For the subject work, the approach of the original work is followed, inclusive of the non-standard designation for the yaw and pitch angles. In this regard, the initial rotation is referenced as the yaw rotation (□) about the initial **Z**-axis (corresponding to the same rotation about the initial **z**-axis if the two frames are coincident prior to the first rotation). The second rotation is referenced as the pitch rotation (□) about the new **y**-axis. The third rotation is referenced as the roll rotation (□) about the new **x**-axis (after the second rotation). Using these three angular definitions, the DCMs associated with a rotation about the **x**-axis, **y**-axis and **z**-axis are:

$$R_{x,\phi} = \begin{bmatrix} 1 & 0 & 0 \\ 0 & +\cos(\phi) & +\sin(\phi) \\ 0 & -\sin(\phi) & +\cos(\phi) \end{bmatrix} \qquad (96)$$

$$R_{y,\theta} = \begin{bmatrix} +\cos(\theta) & 0 & +\sin(\theta) \\ 0 & 1 & 0 \\ -\sin(\theta) & 0 & +\cos(\theta) \end{bmatrix} \qquad (97)$$

$$R_{z,\psi} = \begin{bmatrix} +\cos(\psi) & +\sin(\psi) & 0 \\ -\sin(\psi) & +\cos(\psi) & 0 \\ 0 & 0 & 1 \end{bmatrix} \qquad (98)$$

The composite DCM, based upon equation (95), is:

$${}^{B}R_{G} = R_{x,\phi}R_{y,\theta}R_{z,\psi} \qquad (99)$$

The three elements of the first row of this matrix are +cos(□)cos(□), +sin(□)cos(□) and – sin(□). The three elements of the second row of this matrix are +cos(□)sin(□)sin(□) – sin(□)cos(□), +cos(□)cos(□) + sin(□) sin(□)sin(□) and +cos(□)sin(□). The three elements of the third row are +cos(□)cos(□)sin(□) + sin(□)sin(□), -cos(□) sin(□) + sin(□)sin(□)cos(□) and +cos(□)cos(□). Again, it should be noted that the form of the DCM and its elements will be different if the order of rotations is different.

The next step is the parameterization of the angular velocity vector. To do this, the unit vectors $\mathbf{e}_{□}$, $\mathbf{e}_{□}$ and $\mathbf{e}_{□}$ for the Eulerian local frame are introduced. The angular velocity of the body frame, about the inertial frame, expressed in the components of the Eulerian frame, is the sum of the three Euler angle rate vectors.

$$ {}^{E}_{G}\boldsymbol{\omega}_{B} = \dot{\psi}\mathbf{e}_{\psi} + \dot{\theta}\mathbf{e}_{\theta} + \dot{\phi}\mathbf{e}_{\phi} \tag{100} $$

The unit vector $\mathbf{e}_{[illegible]}$ is a vector in the inertial frame that can be transformed to the body frame after three rotations. For the subject rotation sequence, $\mathbf{e}_{[illegible]} = [0\ 0\ 1]^T = \mathbf{E}_3$. As a result:

$$ {}^{B}\mathbf{e}_{\psi} = {}^{B}R_{G}\mathbf{E}_3 = R_{x,\phi}R_{y,\theta}R_{z,\psi}\mathbf{E}_3 = \begin{bmatrix} -\sin(\theta) \\ +\cos(\theta)\sin(\phi) \\ +\cos(\theta)\cos(\phi) \end{bmatrix} \tag{101} $$

The unit vector $\mathbf{e}_{[illegible]}$ is in an intermediate body frame (B') and requires two rotations to be transformed into the body frame. For the subject rotation sequence $\mathbf{e}_{[illegible]} = [0\ 1\ 0\ ]^T = \mathbf{e}_{2'}$. As a result:

$$ {}^{B}\mathbf{e}_{\theta} = R_{x,\phi}R_{y,\theta}\mathbf{e}_{2'} = \begin{bmatrix} 0 \\ +\cos(\phi) \\ -\sin(\phi) \end{bmatrix} \tag{102} $$

The unit vector $\mathbf{e}_{[illegible]}$ is already in the body frame and $\mathbf{e}_{[illegible]} = [1\ 0\ 0]^T = \mathbf{e}_1$. Therefore the body frame expression of the angular velocity vector is:

$$ \begin{aligned} {}^{B}_{G}\boldsymbol{\omega}_{B} &= \dot{\psi}\begin{bmatrix} -\sin(\theta) \\ +\cos(\theta)\sin(\phi) \\ +\cos(\theta)\cos(\phi) \end{bmatrix} + \dot{\theta}\begin{bmatrix} 0 \\ +\cos(\phi) \\ -\sin(\phi) \end{bmatrix} + \dot{\phi}\begin{bmatrix} 1 \\ 0 \\ 0 \end{bmatrix} \\ &= \begin{bmatrix} -\dot{\psi}\sin(\theta) + \dot{\phi} \\ +\dot{\psi}\cos(\theta)\sin(\phi) + \dot{\theta}\cos(\phi) \\ +\dot{\psi}\cos(\theta)\cos(\phi) - \dot{\theta}\sin(\phi) \end{bmatrix} \end{aligned} \tag{103} $$

This solution, again, will have a different form if the rotation sequence differs. The body frame expression of the angular acceleration is obtained by taking the first body frame derivative of equation (103).

$$ \begin{aligned} {}^{B}_{G}\boldsymbol{\alpha}_{B} &= \frac{{}^{B}d}{dt}{}^{B}_{G}\boldsymbol{\omega}_{B} = {}^{B}_{G}\dot{\boldsymbol{\omega}}_{B} \\ &= \frac{d}{dt}\begin{bmatrix} -\dot{\psi}\sin(\theta) + \dot{\phi} \\ +\dot{\psi}\cos(\theta)\sin(\phi) + \dot{\theta}\cos(\phi) \\ +\dot{\psi}\cos(\theta)\cos(\phi) - \dot{\theta}\sin(\phi) \end{bmatrix} \\ &= \begin{bmatrix} +\ddot{\phi} - \ddot{\psi}\sin(\theta) - \dot{\psi}\dot{\theta}\cos(\theta) \\ \ddot{\psi}\cos(\theta)\sin(\phi) + \ddot{\theta}\cos(\phi) - \dot{\psi}\dot{\theta}\sin(\phi)\sin(\theta) + \\ \dot{\phi}\left(\dot{\psi}\cos(\phi)\cos(\theta) - \dot{\theta}\sin(\phi)\right) \\ \ddot{\psi}\cos(\theta)\cos(\phi) - \ddot{\theta}\sin(\phi) - \dot{\psi}\dot{\theta}\cos(\phi)\sin(\theta) - \\ \dot{\phi}\left(\dot{\psi}\sin(\phi)\cos(\theta) + \dot{\theta}\cos(\phi)\right) \end{bmatrix} \end{aligned} \tag{104} $$

3. ANALYTIC EXAMPLE

In the original work [9], an analytic example was provided, which is considered herein. The following function was used to define the inertial frame translational displacement of body frame center of mass and the Euler angles.

$$ s(t) = s_m\left(\sin(2\pi f_1 t) - \sin(2\pi f_2 t)\right) \tag{105} $$

The first and second time derivatives are readily obtained.

$$ \dot{s}(t) = 2\pi s_m\left(f_1\cos(2\pi f_1 t) - f_2\cos(2\pi f_2 t)\right) \tag{106} $$

$$ \ddot{s}(t) = -4\pi^2 s_m\left(f_1^{\,2}\sin(2\pi f_1 t) - f_2^{\,2}\sin(2\pi f_2 t)\right) \tag{107} $$

The following parameters were provided for the translational motion: (**X**) s_m = 25 in. (0.6350 m), f_1 = 2.0 Hz and f_2 = 3.5 Hz, (**Y**) s_m = 7 in. (0.1778 m), f_1 = 1.0 Hz and f_2 = 5.0 Hz, (**Z**) s_m = 20 in. (0.5080 m), f_1 = 4.0 Hz and f_2 = 2.5 Hz. The following parameters were provided for the Euler angles: ([illegible]) s_m = 20 deg., f_1 = 12 Hz and f_2 = 4.0 Hz, ([illegible]) s_m = 15 deg., f_1 = 7.0 Hz and f_2 = 13 Hz, ([illegible]) s_m = 25 deg., f_1 = 8.0 Hz and f_2 = 0.5 Hz. The body frame referenced translational accelerations were determined at three peripheral locations to simulate three triaxial sensor block readings. These then served as the input to 'reconstruct' the translational and rotational kinematics. Unfortunately, the original reference only provided the distances (i.e. vector magnitudes) of the three points that were used: 3.0, 4.0 and 5.0 inches ($7.62 \cdot 10^{-2}$, $1.016 \cdot 10^{-1}$ and $1.270 \cdot 10^{-1}$ m) respectively. For the reconstruction, these distances were used as constraints in conjunction with the assumption that the body frame origin of coordinates was located at the geometric centroid of the three peripheral point locations. This was expressed as per equation (27). In the original reference [9], numerical integration of equation (36) was achieved using Hamming's modified predictor-corrector method coupled with the use of a Runge-Kutta procedure to start the method. For the subject work, an explicit fourth order Runge-Kutta numerical integration scheme was used for all cases. All mathematical analyses were performed using the Mathematica (v. 12.0; Campaign, Illinois, USA) symbolic mathematics software package. An examination of the figures from the original work revealed that the temporal extent for each plot was approximately 120 milliseconds.

3.1 Prescribed kinematics and angular kinematics

The prescribed inertial frame expressed center of mass accelerations, matching the upper graph of Figure 3 of the original reference (the units of the original are in Gs) is shown in Figure 1.

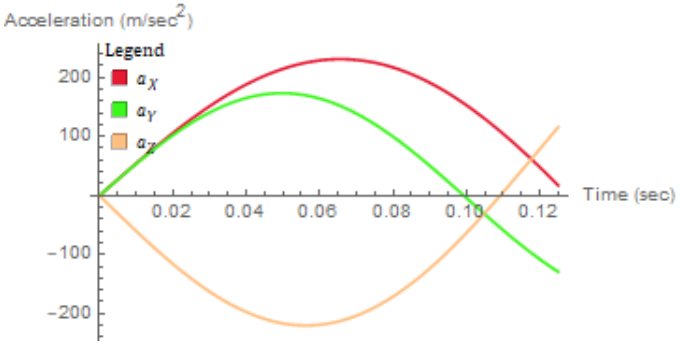

Fig -1: Prescribed inertial frame acceleration-time histories.

The prescribed inertial frame displacement and velocity time histories, matching the graphs shown in Figure 2 of the original reference (distance units of inches in the original), are shown as Figures 2 and 3, herein, respectively.

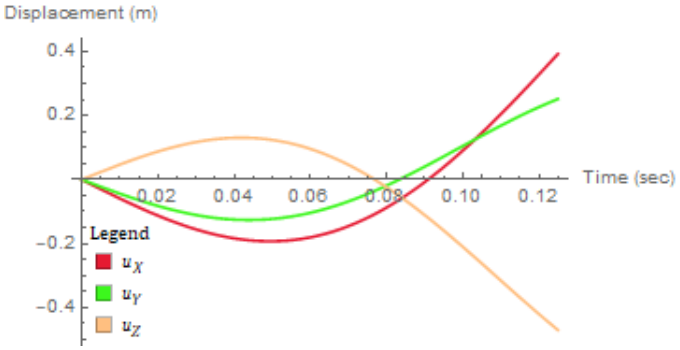

Fig -2: Prescribed inertial frame displacement.

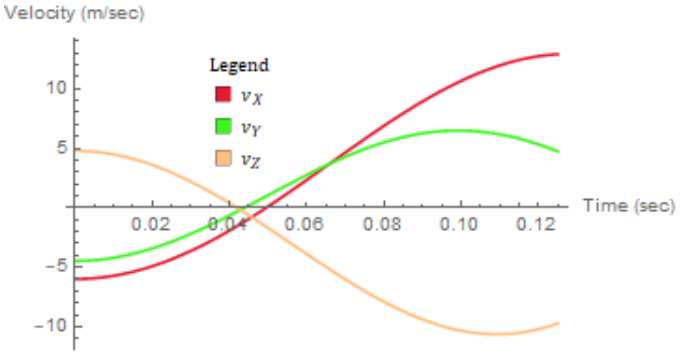

Fig -3: Prescribed inertial frame velocity.

The prescribed Euler angle and Euler rate time-histories are shown in Figures 4 and 5, respectively, and match those shown in Figure 4 of the original reference.

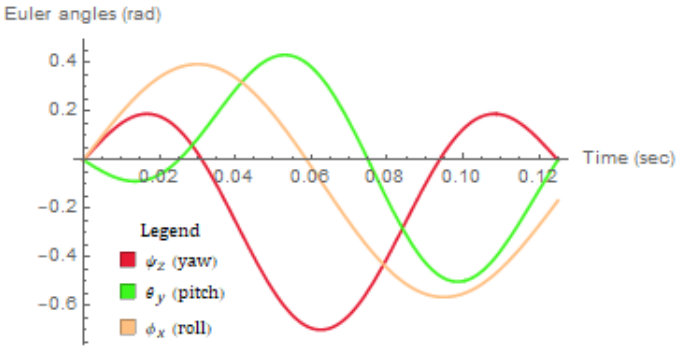

Fig -4: Prescribed Euler angles.

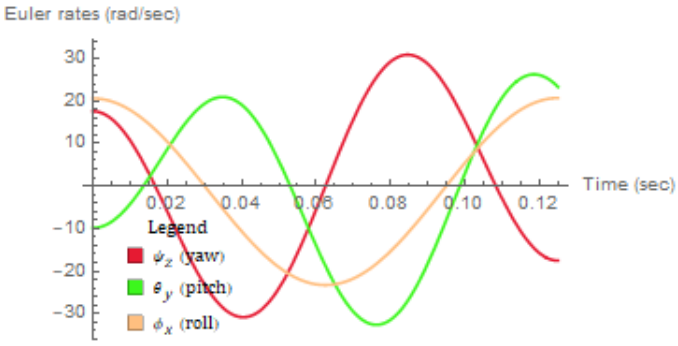

Fig -5: Prescribed Euler rates.

The body frame expression of the angular velocity of the body frame about the inertial frame of reference was obtained by implementing equation (103). The results, shown in Figure 6, matches the results shown in the upper half of Figure 5 of the original reference.

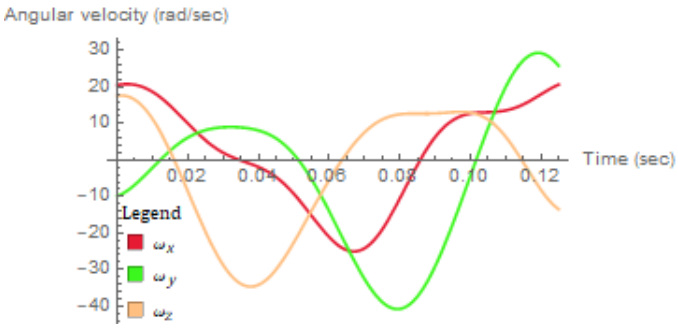

Fig -6: Body frame expressed components of the angular velocity of the body frame about the inertial frame of reference.

The body frame expression of the angular acceleration of the body frame about the inertial frame of reference was obtained by implementing equation (104).

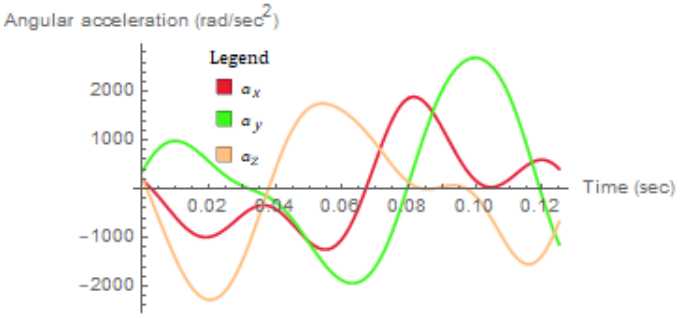

Fig -7: Body frame expressed components of the angular acceleration of the body frame about the inertial frame of reference.

The body frame expressed components of the translational acceleration, shown in Figure 8, match the results shown in bottom half of Figure 3 of the original work and are based upon applying the kinematic transform of ${}^{B}R_{G}$ to the inertial frame expression of the translational acceleration.

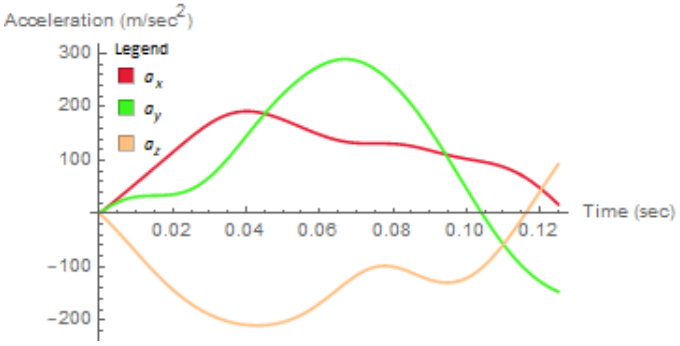

Fig -8: Body frame expressed components of the translational acceleration of the center of mass.

The constraint of the origin of coordinates of the body frame being at the geometric centroid of the triangular plane created by the three peripheral points coupled with the three distance constraints provides for six equations. When three of the nine components of the three peripheral point vectors are known, the remaining components can be determined algebraically. For the subject work, the $\mathbf{e}_1$ and $\mathbf{e}_2$ components of the first position vector were taken as $5.08 \cdot 10^{-2}$ m and $2.54 \cdot 10^{-2}$ m respectively. The $\mathbf{e}_1$ components of both the second and third position vector were taken as $-2.54 \cdot 10^{-2}$ m. The quadratic nature of the vector magnitude function results in a pair of solutions. The first solution set is ${}^{B}\mathbf{r}_1 = \{5.08, 2.54, 5.08\} \cdot 10^{-2}$ m, ${}^{B}\mathbf{r}_2 = \{-2.54, -7.55, 6.31\} \cdot 10^{-2}$ m and ${}^{B}\mathbf{r}_3 = \{-2.54, 5.00, -11.3\} \cdot 10^{-2}$ m. The second solution set is ${}^{B}\mathbf{r}_1 = \{5.08, 2.54, 5.08\} \cdot 10^{-2}$ m, ${}^{B}\mathbf{r}_2 = \{-2.54, -9.58, -2.25\} \cdot 10^{-2}$ m and ${}^{B}\mathbf{r}_3 = \{-2.54, -12.1, -2.83\} \cdot 10^{-2}$ m. The body frame expressed peripheral point accelerations were then generated using equation (17).

3.2 Original method evaluation

For the original method [9], equation (28) was used to reconstruct the body frame translational acceleration of the center of mass and equation (36) was used to solve for the body frame expressed angular acceleration of the body frame about the inertial frame of reference. The overlay plot of the prescribed center of mass translational accelerations, transformed to the body frame, and the reconstructed body frame expressed center of mass translational accelerations, for each set of position vectors, is shown in Figure 9.

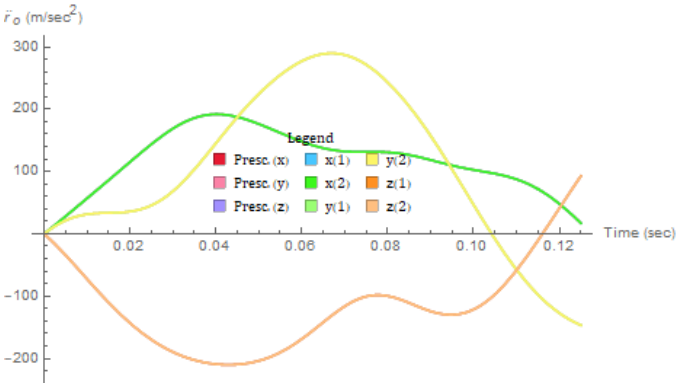

Fig -9: Body frame expressed components of the translational acceleration of the center of mass. In the legend, the abbreviation of Presc. refers to the prescribed acceleration and the axis followed by a number in parentheses refers to the position vector set that was employed.

The overlay plots for the angular acceleration and angular velocity are shown as Figures 10 and 11, respectively. For both the angular acceleration and the angular velocity, the reconstructed curves effectively overlay the analytic curves. This is the expected finding.

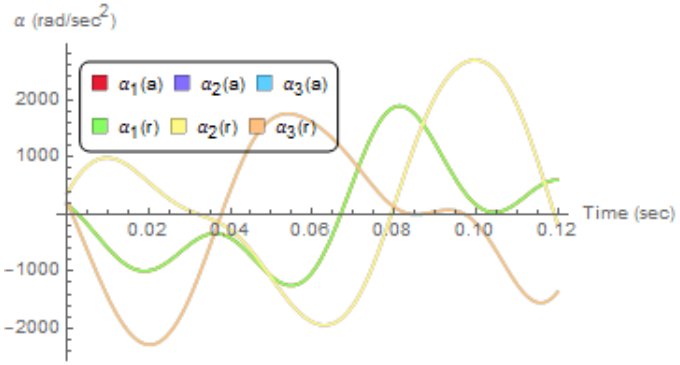

Fig -10: Body frame expressed components of the angular acceleration of the body frame about the inertial frame of reference. In the legend, the parenthetical (a) refers to the analytic approach using equation (104) and the parenetical (r) refers to the reconstructed curve.

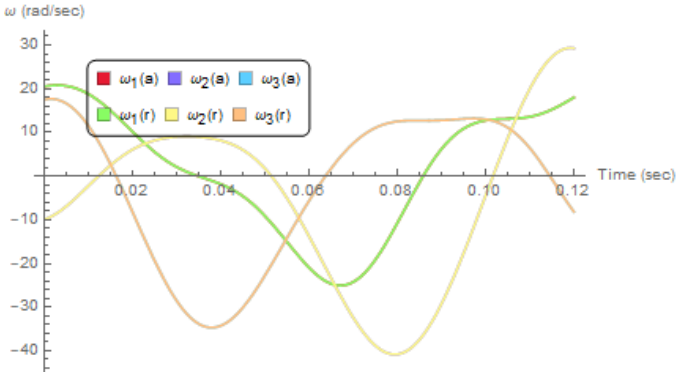

Fig -11: Body frame expressed components of the angular velocity of the body frame about the inertial frame of reference. In the legend, the parenthetical (a) refers to the analytic approach using equation (103) and the parenthetical (r) refers to the reconstructed curve.

3.3 Updated method evaluation

For the updated formulation, the solution from equation (67) contained both the translational acceleration and angular acceleration. The results for the center of mass translational acceleration are shown in Figure 12.

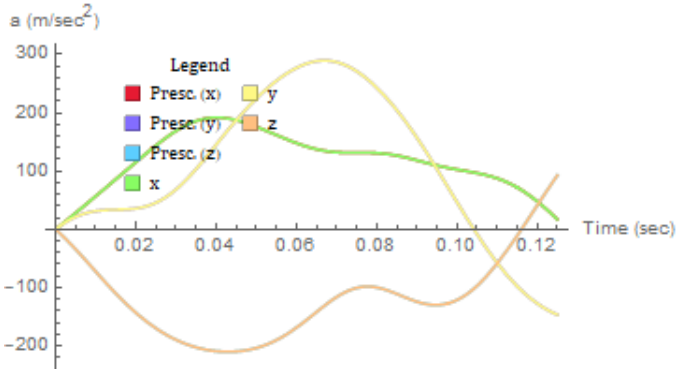

Fig -12: Body frame expressed components of the translational acceleration of the center of mass. In the legend, the abbreviation of Presc. refers to the prescribed acceleration.

The results for the angular acceleration and angular velocity are shown in Figures 13 and 14, respectively. Again, as expected, the reconstructed curves overlay the analytic curves.

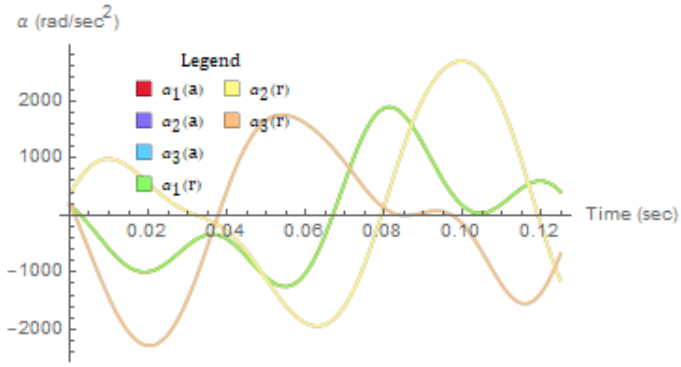

Fig -13: Body frame expressed components of the angular acceleration of the body frame about the inertial frame of reference. In the legend, the parenthetical (a) refers to the analytic approach and (r) refers to the reconstructed approach.

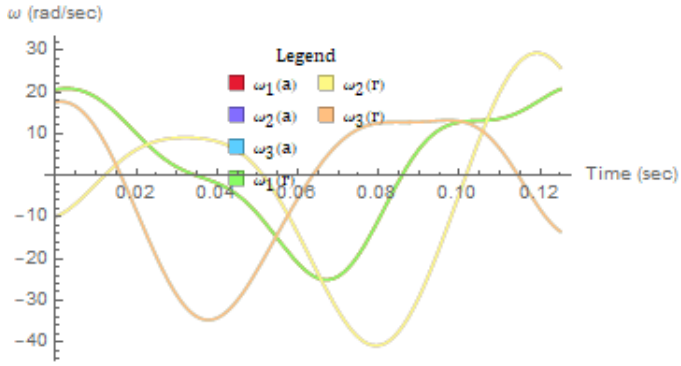

Fig -14: Body frame expressed components of the angular velocity of the body frame about the inertial frame of reference. In the legend, the parenthetical (a) refers to the analytic approach and (r) refers to the reconstructed approach.

3.4 Non-centroidal center of mass example

For the purpose of a preliminary evaluation of the violation of the assumption of the body frame origin of coordinates being located at the geometric centroid of the peripheral sensor locations, the **x**-axis position of the first peripheral sensor location was increased by 20 percent while leaving all other position vector components unchanged. The results of the reconstructed body frame expressed translational acceleration components of the center of mass are shown in Figures 15-17.

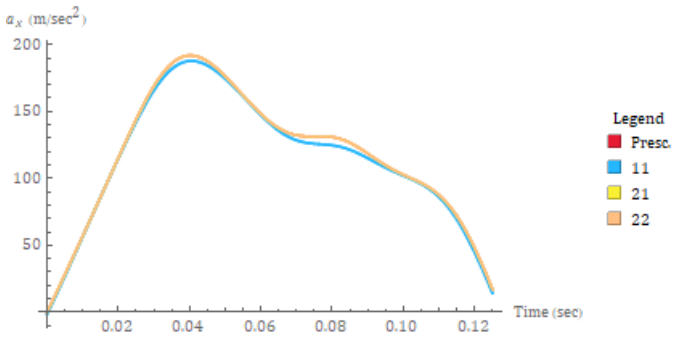

Fig -15: Body frame expressed **x**-axis center of mass translational acceleration. In the legend, Presc. Refers to the prescribed acceleration, 11 refers to the original method, 21 refers to the updated method using the first set of position vectors and 22 refers to the updated method using the second set of position vectors.

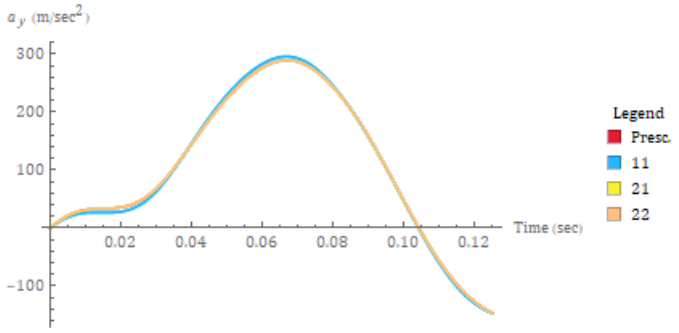

Fig -16: Body frame expressed **y**-axis center of mass translational acceleration. The legend follows Figure 15.

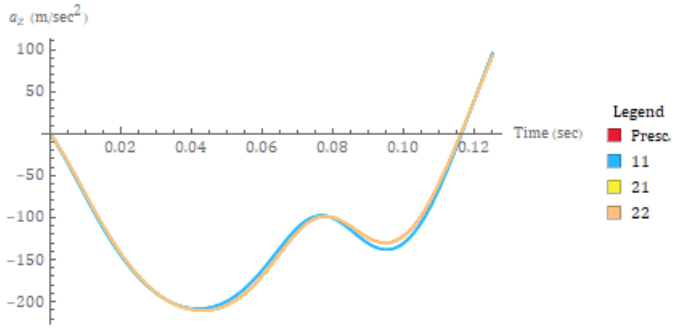

Fig -17: Body frame expressed **z**-axis center of mass translational acceleration. The legend follows Figure 15.

Figures 18-20 show the overlay plots for the body frame expressed components of the angular acceleration vector of the body frame about the inertial frame of reference.

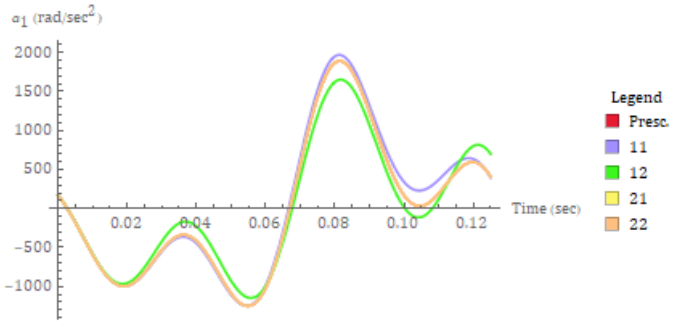

Fig -18: Body frame expression of the angular acceleration of the body frame about the inertial frame of reference around the **x**-axis. The legend follows Figure 15 but with 12 denoting the original method using the second set of position vectors.

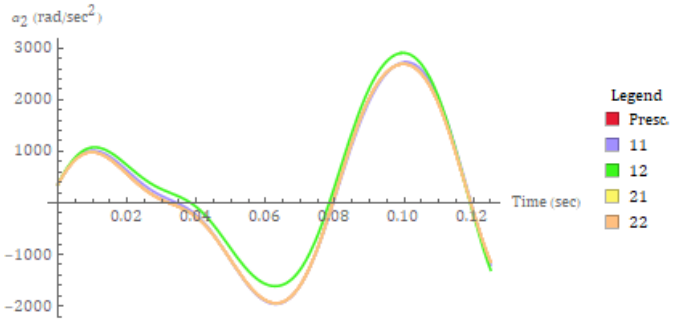

Fig -19: Body frame expression of the angular acceleration of the body frame about the inertial frame of reference around the **y**-axis. The legend follows Figure 18.

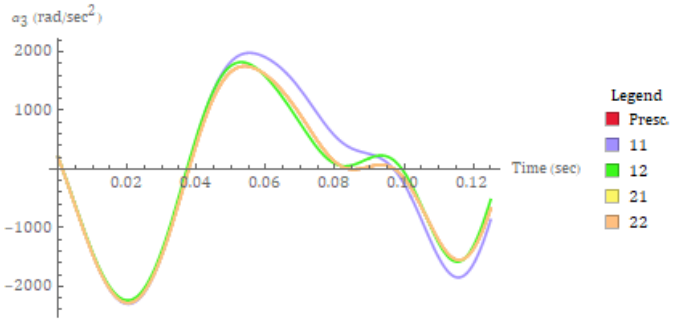

Fig -20: Body frame expression of the angular acceleration of the body frame about the inertial frame of reference around the **z**-axis. The legend follows Figure 18.

Figure 21-23 show the overlay plots for the body frame expressed components of the angular velocity vector of the body frame about the inertial frame of reference.

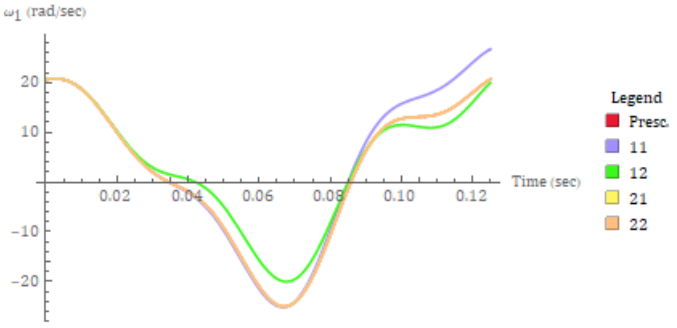

Fig -21: Body frame expression of the angular velocity of the body frame about the inertial frame of reference around the **x**-axis. The legend follows Figure 17.

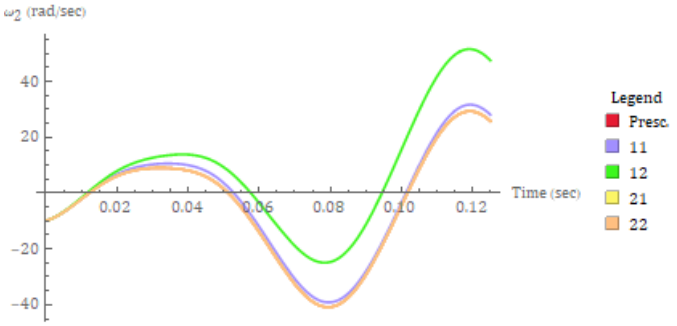

Fig -22: Body frame expression of the angular velocity of the body frame about the inertial frame of reference around the **y**-axis. The legend follows Figure 18.

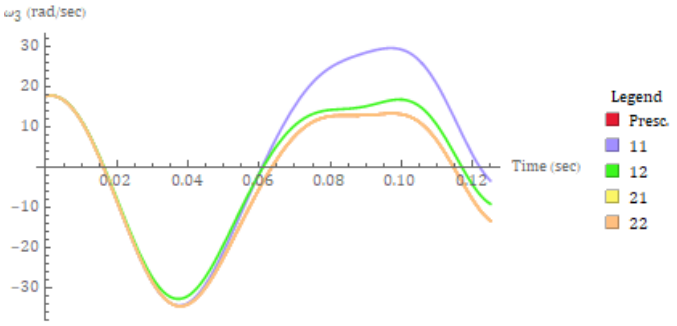

Fig -23: Body frame expression of the angular velocity of the body frame about the inertial frame of reference around the **z**-axis. The legend follows Figure 18.

4. DISCUSSION

The accurate quantification of injury metrics, irrespective of the context necessitating such quantification, is predicated, in part, upon the accurate determination of the system response parameters that deterministically serve as the independent variables in the injury metric or metrics under consideration. For the case of closed head injury, the available, commonly utilized injury metrics can readily be placed into one of two categories. The first category consists of metrics that are based upon a certain singular value of a particular kinematic response (e.g. peak directional head center of mass translational acceleration) or upon a portion, up to the whole, of the time history for a particular kinematic response (e.g. average directional head center of mass translational acceleration). The second category consists of functions of one or more kinematic response parameters (e.g. the Head Injury Criterion). When the translational acceleration of the head is a required, either as a direct injury metric or as a requisite for calculating an injury metric, the location at which the translational acceleration is required is at the head center of mass. When an ATD is used as a test subject, the head center of mass translational acceleration can directly be measured. Such direct measurement, clearly, cannot be done in a non-invasive manner when using live test subjects or cadaveric test subjects. In such cases, the use of peripherally positioned sensors is generally requisite if test subject fixed measurements are used.

The focus of the subject work was the presentation, extension and evaluation of one peripheral sensor array. This array consists of three peripherally arranged triaxial accelerometer blocks and with each sensor block comprised of three uniaxial translational accelerometers arranged in a mutually orthogonal manner. The original work on using this array for determining the angular kinematics and center of mass (for the object, such as the head, to which the array is attached) translational kinematics was developed with a key limiting assumption. This assumption, represented mathematically by equation (27), was of the body frame origin of coordinates being located at the geometric centroid of the plane defined by the three peripheral sensor block locations. The result of this assumption is the simplification that the body frame expressed center of mass translational acceleration, as given by equation (28), is simply the average of the accelerations as measured at the three peripheral locations.

The validity of the underlying assumption was evaluated using an idealized hypothetical example in which the center of mass inertial frame expressed translational displacement and the angular displacements of the Euler angles were prescribed. Three peripheral locations were chosen such that the above-referenced position constraint was satisfied. The calculated accelerations at the three peripheral points were determined using standard rigid body kinematics equations and these accelerations were then used to reconstruct the center of mass translational acceleration and the angular kinematics. The reconstructed results, as expected, closely matched the prescribed kinematics, as shown by Figures 9-11.

The extension of the original formulation was achieved by eliminating the assumption of the body frame origin of coordinates being colocated at the geometric centroid of the plane formed by the three peripheral sensor block locations and then solving the six coupled equations obtained from minimizing the sum of squared errors with respect to each of the six system unknowns (the three body frame expressed center of mass translational acceleration components and the three body frame expressed components of the angular acceleration of the body frame about the inertial frame of

reference). The extended method, also as expected, produced reconstructed results, as shown by Figures 12-14, that closely matched the prescribed kinematics of the idealized hypothetical example from the originating study.

The second idealized hypothetical example was evaluated as a preliminary exploration of the errors engendered by the violation of the assumption in question and was not intended to equate to or replace a formal error analysis. In this regard, the idealized hypothetical example from the originating study was slightly modified by changing a single factor. This factor was the **x**-axis location of one sensor block and the degree of modification was increasing the position by 20 percent. The extended approach reproduced both the translational acceleration as shown in Figures 15-17 and both the angular acceleration, as shown in Figures 18-20, as well as the angular velocity, as shown in figure 21-23. The original method, however, failed to accurately reproduce the prescribed kinematics and with a degree of deviation commensurate with the extent upon which the kinematic response depended upon the position of the sensor block along the specified body frame axis.

There is clearly room for additional work for which the subject research can readily be viewed as a springboard. The first prong clearly consists of performing a formal error analysis in order to ascertain the full scope of potential errors engendered by deviating from the previously expressed assumption of the original work. The second prong consists of evaluating actual test data. One may readily appreciate that additional factors such as measurement noise and the signal filtering paradigm employed may readily impact upon the accuracy of any analytic method employed for determining the relevant kinematic responses. Finally, the third prong of additional research stems from the application of the further extension of the theoretical framework, which was developed in Sections 2.5 through 2.7, based upon the use of four triaxial linear accelerometer block sensors (each sensor block comprised of accelerometers arranged in a mutually orthogonal configuration).

REFERENCES

[1] C. Gadd (1966) "Use of a weighted-impulse criterion for estimating injury hazard." Society of Automotive Engineers Technical Paper No. 660793.

[2] W. Fan (1971) "Internal head injury assessment." Society of Automotive Engineers Technical Paper No. 710870.

[3] J. Newman (1986) "A generalized acceleration model for brain injury threshold (GAMBIT)." Proceedings: International Research Council on the Biomechanics of Injury (IRCOBI); Zurich, Switzerland, September 2-4, 1986.

[4] J. Newman, N. Shewchenko and E. Welbourne (2000) "A proposed new biomechanical head injury assessment function – the maximum power index." Stapp Car Crash Journal 44: 215-247.

[5] E. Takhounts, M. Craig, K. Moorhouse and J. McFadden (2013) "Development of Brain Injury Criteria (BrIC)." Stapp Car Crash Journal 57: 243-266.

[6] Procedures for assembly, disassembly and inspection (PADI) of the Hybrid III 50th percentile dummy's nine accelerometer array head (NAAH) with redundant head c.g. accelerometers (2001) US Department of Transportation, National Highway Traffic Safety Administration, Washington, DC, USA.

[7] A. Padgaonkar, K. Krieger and A. King (1975) "Measurement of angular acceleration of a rigid body using linear accelerometers." Journal of Applied Mechanics 42: 552-556.

[8] N. Yoganandan, J. Zhang, F. Pintar and Y. Liu (2006) "Lightweight low-profile nine-accelerometer package to obtain angular accelerations in short-duration impacts." Journal of Biomechanics 39(7): 1347-1354.

[9] N. Alem and G. Holstein (1977) "Measurement of 3-D motion." Presented: 5th International Workshop on Human Subjects for Biomechanical Research; New Orleans, Louisiana. Also: University of Michigan Highway Safety Research Institute publication UM-HSRI-77-46.

[10] F. Bendjellal, L. Oudenard, J. Uriot, C. Brigout and F. Brun-Cassan (1990) "Computation of Hybrid III head dynamics in various impact situations." Society of Automotive Engineers Technical Paper No. 902320.

[11] T. Szabo, J. Welcher, R. Anderson, M. Rice, J. Ward, L. Paulo and N. Carpenter (1994) "Human occupant kinematic response to low speed rear-end impacts." Society of Automotive Engineers Technical Paper No. 940532.

[12] T. Szabo and J. Welcher (1996) "Human subject kinematics and electromyographic activity during low speed rear impacts." Society of Automotive Engineers Technical Paper No. 962432.

[13] R.D. Anderson, J. Welcher, T. Szabo, J. Eubanks, W. Haight (1998) "Effect of braking on human occupant and vehicle kinematics in low speed rear-end collisions." Society of Automotive Engineers Technical Paper No. 980298.

[14] M. Ivory, C. Furbish, M. Hoffman, E. Miller, R.L. Anderson and R.D. Anderson (2010) "Brake pedal response and occupant kinematics during low speed rear-end collisions." Society of Automotive Engineers Technical Paper No. 2010-01-0067.

[15] R. Bjehin (1957) "A comparison between the Frankfort horizontal and the sella turcica-nasion as reference planes in cephalometric analysis." Acta Odontologica Scandanavica 15(1): 1-12.

[16] E. El Kattan, M. El Kattan and O. Elhiny (2018) "A new horizontal plane of the head." Open Access Macedonian Journal of Medical Sciences 6(5): 767-771.

[17] N. Yoganandan, F. Pintar, J. Zhang and J. Baisden (2009) "Physical properties of the human head: mass, center of gravity and moment of inertia." Journal of Biomechanics 42(9): 1177-1192.

[18] L. Walker and U. Pontius (1973) "Mass, volume, center of mass and mass moment of inertia of head and head and neck of human body." Society of Automotive Engineers Technical Paper No. 1973-02-01.

[19] R. Jazar (2011) Advanced dynamics: rigid body, multibody and aerospace applications. Hoboken, New Jersey, USA: John Wiley & Sons, Inc.

[20] J. Singh (2020) "Planar rigid body motion extraction from motor vehicle collision testing conducted under United States safety testing protocols." International Research Journal of Engineering and Technology 7(7): 1169-1190.

[21] S. Park and S, Hong (2011) "Angular rate estimation using a distributed set of accelerometers." Sensors 20(11): 10444-10457.

BIOGRAPHY

Mr. Singh is a private practice engineer with specialties in the fields of motor vehicle accident reconstruction and biomechanical engineering. He holds a BS in mechanical engineering from the University of Illinois at Urbana-Champaign and a MS in biomedical engineering from the University of Southern California. He has also authored numerous other peer reviewed conference proceedings, technical papers and scientific papers.